Optical Properties of Conducting Polymers

A. O. PATIL, A. J. HEEGER,* and F. WUDL*

Institute for Polymers and Organic Solids and Department of Physics, University of California, Santa Barbara, California 93106

Received June 25, 1987 (Revised Manuscript Received September 10, 1987)

Contents

I. Introduction

A. Conducting Polymers as a Growing Class of Electronic Materials

Interest in conducting polymers as a new class of electronic materials began with the preparation of $(CH)_x$ in the form of shiny coherent films, with the discovery that polyacetylene could be doped by charge-transfer reactions with an oxidizing or reducing agent,[1] and with the discovery that the doped polymer exhibits a dramatic increase in conductivity with values in the metallic regime. The study of these materials has generated entirely new scientific concepts as well as the potential for new technology.[2]

Organic conducting polymers have a highly anisotropic quasi-one-dimensional structure similar, in some aspects, to that of charge-transfer salts. In the conducting state, both these types of materials are ionic. In charge-transfer complexes, conductivity is greater along the stacking direction (due to π–π overlap between successive molecules in the one-dimensional stack) while in conducting polymers conductivity is higher along the chain direction (due to π–π overlap between successive monomers in the one-dimensional chain). In conducting polymers, the chainlike structure leads to strong coupling of the electronic states to conformational excitations (solitons, polarons, bipolarons, etc.) peculiar to one-dimensional systems. The relatively weak interchain binding allows diffusion of dopant molecules into the structure (between chains), while the strong intrachain carbon–carbon bonds maintain the integrity of the polymer.

Conducting polymers can be broadly divided into two types, namely, those with a degenerate ground state and solitons (see below) as the important excitations and those where the ground-state degeneracy is lifted so that polarons and bipolarons (see section IIIB) are the important excitations and the dominant charge-storage configurations. Polyacetylene, $(CH)_x$, is the extensively studied example with a degenerate ground state (the double and single bonds can be interchanged with no cost of energy). Poly(*p*-phenylene), poly(*p*-phenylene sulfide), and polyheterocycles (polypyrrole, polythiophene, etc.) each have a nondegenerate ground state (for example, in poly(*p*-phenylene) the quinoid form has a higher energy than the benzenoid form).

B. Summary of Physical Properties

1. Polyacetylene

Polyacetylene is the simplest conjugated conducting polymer. It consists of weakly coupled chains of CH units forming a pseudo-one-dimensional lattice. Both the cis and trans forms can be prepared as silvery flexible films which can be made either free-standing or on a substrate with thickness varying[3] from 10^{-5} to 0.5 cm. The trans isomer is the thermodynamically stable form. Any cis:trans ratio can be maintained at low temperature, but complete isomerization from *cis*- to *trans*-$(CH)_x$ can be accomplished after synthesis by heating the film to temperatures above 150 °C from a few minutes to more extended time periods.[4,5] It can also be prepared in pure trans form at room temperature.[5a]

Electron microscopy studies show[3,6,7] that the as-grown $(CH)_x$ films consist of randomly oriented fibrils of ~20-nm diameter. The films can be stretch-oriented to in excess of 5 times their original length with concomitant partial alignment of the fibrils.[6,8,9] The nominal bulk density is 0.4 g cm^{-3} compared with the 1.2 g cm^{-3} obtained by flotation techniques.[10] Therefore,

0009-2665/88/0788-0183$06.50/0

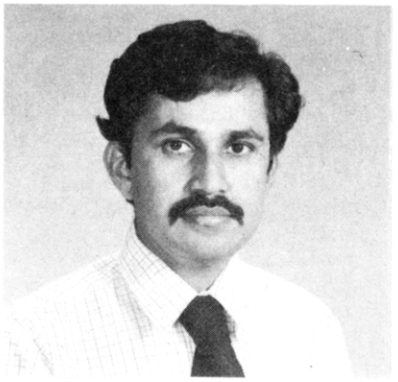

Abhimanyu O. Patil is a native of India. He received his Ph.D. degree from the Indian Institute of Technology, Bombay, in organic polymer chemistry while working with Dr. S. S. Talwar. After initial postdoctoral work in solid-state organic chemistry at the University of Illinois, Urbana, with Drs. David Y. Curtin and Iain C. Paul, he joined Professor Fred Wudl's group at the Institute for Polymers and Organic Solids, University of California, Santa Barbara. His research interests are in conducting polymers, polymer chemistry, and synthetic and solid-state organic chemistry.

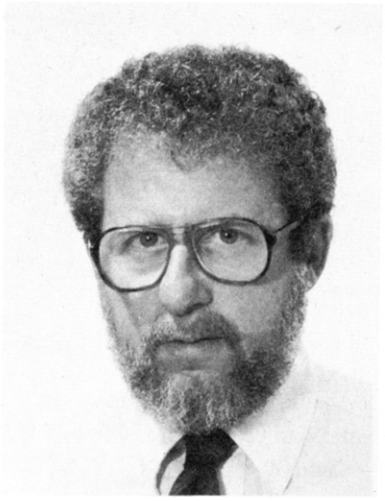

Professor Alan J. Heeger received his Ph.D from the University of California, Berkeley, in 1961. He then went to the University of Pennsylvania and was made Professor of Physics in 1967. He served at Pennsylvania for 21 years as Professor, as Director of the Laboratory for Research on the Structure of Matter (1972–1980), and as Vice-Provost for Research (Acting, 1980–1981). Professor Heeger joined the faculty at the University of California, Santa Barbara, in 1982 as Professor of Physics and Director of the Institute for Polymers and Organic Solids. Professor Heeger and his colleagues at UCSB have done pioneering research in the area of highly conducting organic solids. His current interests lie in the development of the fundamental physics and chemistry which determine the electronic and magnetic properties of semiconducting and metallic polymers with a goal of making these novel materials available for technological applications.

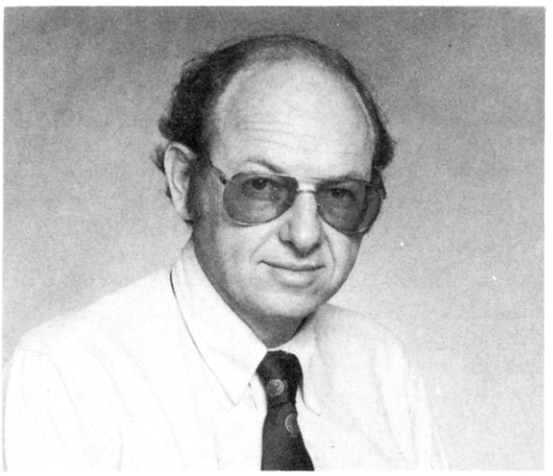

Since 1982, Fred Wudl has been Associate Director of the Institute for Polymers and Organic Solids and Professor in the departments of Chemistry and Physics at the University of California at Santa Barbara. Prior to that he was a Member of the Technical Staff for approximately 10 years at Bell Laboratories in Murray Hill, NJ. He went to Bell after spending 1 year as a postdoctoral fellow at Harvard University and 4 years as an Assistant Professor in the Department of Chemistry at SUNY/Buffalo. He obtained his Ph.D. degree from the University of California at Los Angeles in 1967. His current interests are in all aspects of the organic solid state, encompassing crystalline molecular solids and polymeric materials. In the past few years, his group has focused their effort on conducting polymers and charge-transfer complexes of heterocyclic molecules.

the polymer fibrils fill only about one-third of the total volume and the effective surface area is quite high (~60 m^2/gm). X-ray studies show that the $(CH)_x$ films are highly crystalline (≈80%).[11,12]

The electrical conductivity of polyacetylene can be varied in a controlled manner over 15 orders of magnitude through chemical or electrochemical doping. Figure 2 shows electrical conductivity of doped *trans*-$(CH)_x$ films as a function of dopant concentration. Recent studies have reported conductivities as high as[5b] 1.5×10^5 S/cm (comparable to that of copper), with indications that the intrinsic conductivity may be considerably greater.

The carriers generated by the doping of $(CH)_x$ result from charge transfer. Charge transfer occurs from polymer to acceptor (A), with the polymer chain acting as a polycation in the presence of A^- species. For a donor (D), the polymer chain acts as a polyanion in the presence of D^+ species. The A^- or D^+ ions reside between polymer chains. Chemical compensation has been demonstrated, implying that the doping is reversible. Reversible doping can also be carried out electrochemically. In this case the polymer is used as the working electrode; upon oxidation or reduction, the counterions enter the structure (between chains) from the electrolyte. The reversibility implies that the $(CH)_x$ chains remain intact in the doped polymer; this has been verified in detail through structural studies.

If the bond lengths in pure *trans*-$(CH)_x$ were uniform, the polymer would be a quasi-one-dimensional metal with a half-filled band. Such a system is unstable with respect to a dimerization distortion (the Peierls instability)[13,14] in which adjacent CH groups move toward each other forming alternately short (partial double) bonds and long (partial single) bonds, thereby lowering the energy of the system. Clearly, by symmetry, the double and single bonds may be interchanged without altering the energy. Thus, there are two lowest energy states, A and B, having two distinct bonding structures (Figure 29). This two fold degeneracy leads to the existence of nonlinear topological excitations (bond alternation domain walls or solitons) which appear to be responsible for many of the remarkable properties of $(CH)_x$.[15-20]

The proposed soliton in $(CH)_x$ is a topological kink in the electron–lattice system: a bond alternation do-

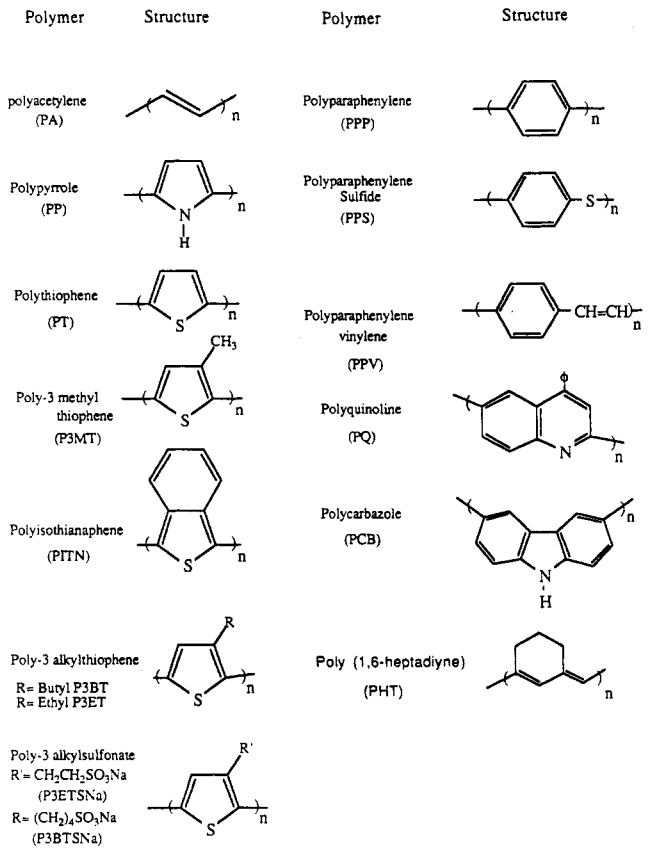

Figure 1. The principal conducting polymers.

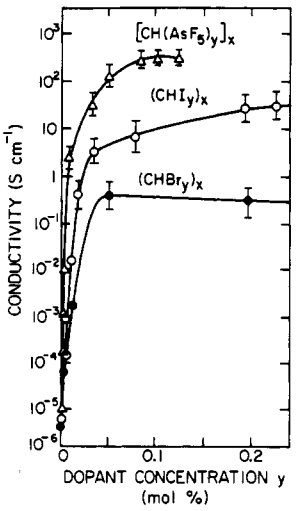

Figure 2. Electrical conductivity of doped *trans*-$(CH)_x$ film as a function of dopant concentration.

main wall connecting A and B phases with opposite-bond alternation (see Figure 29b). Since there is complete degeneracy (the kink can be anywhere) and since the mass is small, the kink is expected to be mobile.[2a] The competition of elastic and condensation energies spreads the domain wall over a region of about $15a$, where a is the C–C distance along the $(CH)_x$ chain.

For a more detailed review of the physical properties of polyacetylene and their interpretation in terms of the soliton model (and other models) the reader is referred to ref 2a.

2. Polypyrrole

Among the conducting polyheterocycles, the most intensively studied polymers are polypyrrole, polythiophene, and their derivatives as well as polyphenylene and polyphenylene chalcogenides. Polypyrrole was shown to be a conducting polymer in 1968. Dall'Olio et al.[21] prepared it by oxidation of pyrrole in sulfuric acid as a black powder with room temperature conductivity of 8 S cm^{-1}. This work was then extended by workers at IBM who showed that films of this polymer can be obtained by electrochemical polymerization.[22] These films could be cycled electrochemically between a conducting (doped) state and an insulating state, with conductivities varying from[22] 100 to 10^{-10} S cm^{-1}. Unlike the morphology of the Shirakawa polyacetylene, which is fibrillar, polypyrrole films are dense. Thus, physically impermeable films of polypyrrole could be prepared.

3. Polythiophene

Polythiophene and its derivatives are stable both in their doped and in their undoped states. The most important aspect of this heterocycle is the ease of 3-substitution, which can be used to prepare new polymers with exciting properties. By substituting long flexible chains in the 3-position, one can decrease the interchain interaction and achieve high solubility (and processibility) with some sacrifice in conductivity. Several organic solvent soluble and even water-soluble 3-substituted polythiophenes with high conductivities have been prepared. For example, poly(3-hexylthiophene) has a room temperature conductivity of 30 S cm^{-1}. Poly(3-methylthiophene) has much higher conductivity ($\sigma \simeq 500$ S cm^{-1}). It has been reported[23] that certain substituted polythiophenes with conductivities above 1000 S cm^{-1} can be prepared. The parent polythiophene has a room temperature conductivity of 50–100 S cm^{-1}.

Molecular design concepts resulted in the modification of polythiophene; by benzannelation, a new polymer, poly(isothianaphthene), was synthesized with the smallest band gap among all conjugated conducting polymers. This polymer has a band gap of 1 eV compared with the parent polythiophene, which has a band gap of 2 eV.

C. Electronic Spectroscopy

The high-contrast electrochromic phenomenon associated with electrochemical doping and the nearly identical spectral changes which occur on chemical doping are of particular interest. The characteristic changes in absorption spectrum sketched in Figure 3 appear to be general features of conducting polymers. The oscillator strength associated with the interband transition (prior to doping) shifts into the free carrier contribution in the infrared (after doping). The effect of such spectral changes depends initially on the magnitude of the energy gap (E_g). If E_g is greater than 3 eV, the undoped insulating polymer is transparent (or lightly colored) whereas after doping, the conducting polymer is typically highly absorbing in the visible. If, however, E_g is small (~1–1.5 eV), the undoped polymer

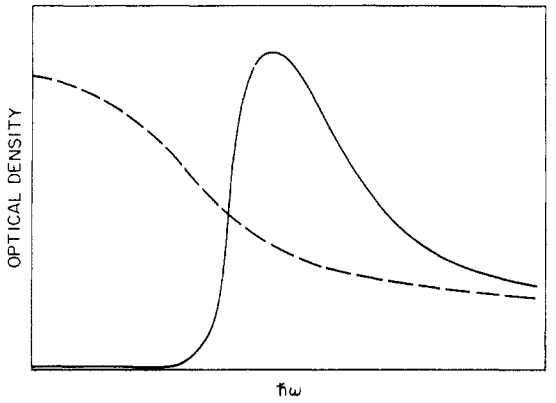

Figure 3. Schematic diagram of optical density of a conducting polymer as a function of photon energy. Solid curve, neutral polymer (semiconductor), which is transparent for $\hbar\omega < E_g$; dashed curve, heavily doped polymer (metallic).

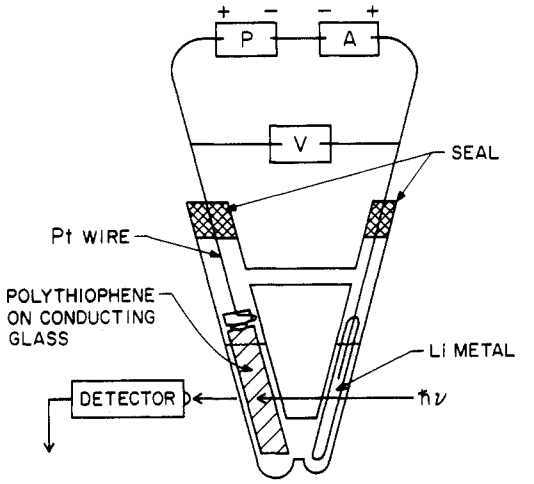

Figure 4. Diagram of apparatus used for in situ visible–IR absorption measurements during electrochemical doping.

will be highly absorbing, whereas after doping, the free carrier absorption can be relatively weak in the visible *provided* the typical carrier scattering time (and mean free path) is sufficiently long.

The optical properties of a conducting polymer are important to the development of an understanding of the basic electronic structure of the material. The π conjugation in the polymers is implied by their color and their electronic spectra; thus spectroscopy is a powerful probe for characterization of the electronic processes that occur in the polymer in the undoped and doped states, as well as during doping. The changes of the optical spectra accompanying doping are significant, and these spectral changes have played a key role in elucidating the mechanism of doping and the nature of the charge-storage species in the polymer chain. In this review we summarize the optical studies of some of the key conducting organic polymers that have become important in recent years. We focus primarily on the polymer systems studied in the Institute for Polymers and Organic Solids at UCSB. Parallel studies on these and related systems have been carried out in many laboratories throughout the world.[2]

The experimental technique of in situ optoelectrochemical spectroscopy is described in section II, and the spectroscopic data for a number of the most-studied polymers are summarized in section III. These results are put into a theoretical context in section IV, where we summarize the concepts of charge storage in solitons, polarons, and bipolarons and the associated spectroscopic signatures.

II. Experimental Setup for In Situ Optoelectrochemical Spectroscopy

This technique[24,25] utilizes an electrochemical cell with the polymer under study as the working electrode, a counter electrode, a reference electrode, and an appropriate electrolyte in solution in a solvent that has an electrochemical window compatible with the oxidation and/or reduction potentials of the polymer. The in situ technique has been adapted to study many different properties of conducting polymers, e.g., spectroscopy, electron spin resonance, and structure (through X-ray diffraction). The details of the cell design depend on the specific use. In the case of in situ optical studies the cell is designed to minimize light scattering and to optimize light throughput (rectangular cell, semitransparent, electrode, etc.); for in situ electron spin resonance studies, the cell must fit inside the microwave cavity of an ESR spectrometer.

A Pyrex cell was designed and constructed so that the visible to near-IR spectra of a conducting polymer (e.g., polyacetylene, polythiophene) could be recorded in situ throughout the electrochemical doping and/or undoping process. A schematic diagram is shown in Figure 4; the glass cell contains a Pt-metal strip, polymer sample on an indium/tin oxide (ITO) conducting glass, and Ag/Ag^+ or Li reference electrode. The electrolyte solution, 0.1 *m* Bu_4NClO_4 in acetonitrile, completes the internal circuit. The cell is thin and of rectangular cross section in order to minimize scattered light, to prevent divergence of the beam, and to minimize the ratio of the electrolyte to polymer volumes. The cell is sealed with the Pt wires extending through the seals. A piece of conducting glass is also mounted in the cell without polymer film for a reference determination of background absorption. The experimental setup is quite general and can be carried out with any monochromator and a microcomputer.

In a typical experiment the reference sample is run first to obtain an effective "source" spectrum I_0 involving all absorptions not due to the polymer. The data are stored in the computer. The sample-containing portion of the cell is rigidly mounted in the light path so that a single area of the polymer film is in the beam throughout the doping–undoping cycle, thus allowing quantitative in situ comparison of the spectra for each voltage (i.e., each dopant concentration). The raw transmission data (I_t) as well as the optical density [$-\ln (I_t/I_0)$] are stored in the computer for each value of the applied voltage. The data are typically analyzed in terms of the optical density or absorption coefficient, $\alpha = (1/d)$ in (I_t/I_0), where d is the sample thickness.

The voltage across the cell is set to the desired value, and the cell is allowed to come to equilibrium. During this time, the monochromator is set at λ_{max}, and the strength of the band-gap transition $\alpha(\omega)$ (absorptivity) is monitored along with the cell current. Initially, after stepping the external voltage, current flows and then decays steadily with time as the cell approaches equi-

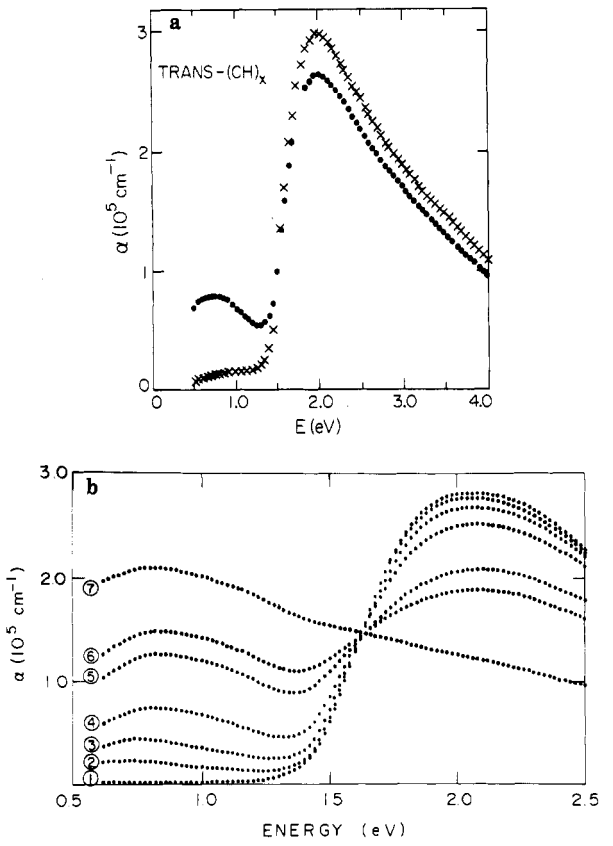

Figure 5. (a) Absorption coefficient of *trans*-$(CH)_x$: (×) before doping; (●) after doping to a fraction of a percent by exposure to AsF_5 vapor. See ref 37. (b) In situ absorption curves for *trans*-$(CH)_x$ during electrochemical doping with ClO_4^-. The applied cell voltages (relative to Li) and corresponding concentrations are as follows: curve 1, 2.2 V ($y = 0$); curve 2, 3.28 V ($y \approx 0.003$); curve 3, 3.37 V ($y \approx 0.0065$); curve 4, 3.46 V ($y \approx 0.012$); curve 5, 3.57 V ($y \approx 0.027$); curve 6, 3.64 V ($y \approx 0.047$); curve 7, 3.73 V ($y \approx 0.078$). See ref 24.

librium. Correspondingly, the absorption coefficient changes continuously after a voltage step and approaches a steady value characteristic of the new dopant concentration. By monitoring the approach to equilibrium through $\alpha(t)$, one can obtain direct information on the kinetics of the charge-transfer reaction (in addition to the spectra at equilibrium). After these parameters reach steady state, a spectrum is taken, and the process is repeated at successive cell voltages until the entire doping range has been covered.

III. Spectroscopic Results for Specific Conducting Polymers

A. Polyacetylene

The visible spectrum of *trans*-polyacetylene film shows a strong absorption band with λ_{max} at 1.9 eV and a band gap of about 1.4 eV. The cis isomer has a similar spectrum with slightly higher energies. The λ_{max} absorption in the polymer corresponds to a π–π^* transition from the valence band to the conduction band. Polyacetylene can be doped with various electron acceptors such as AsF_5, I_2, Br_2, BF_3, HF, and $HClSO_3$ as well as by electron donors such as Li, Na, and K; in all cases the spectral changes are essentially the same. Although one would like to make a direct comparison of the doping-induced spectral changes of *cis*-$(CH)_x$ and *trans*-$(CH)_x$, this is not possible, since while doping, *cis*-polyacetylene undergoes isomerization to the trans isomer.[26]

The interesting observation that on doping polyacetylene (with I_2 or AsF_5), the intensity of the interband transition decreased and, simultaneously, a new intense absorption appeared in the near-IR at an energy of about half the initial interband transition was recorded in 1980.[37] This "mid-gap" transition was shown to be a general feature of doped polyacetylene, independent of dopant, and independent of whether the dopant was n-type (reduction) or p-type (oxidation).[30c] Although the initial experiments utilized chemical doping, the most elegant and quantitative way to study the effect of doping on the optical properties is by use of optoelectrochemical spectroscopy, as described above.[25]

Electrochemical studies[27,28] have allowed precise control of the doping process and quantitative measurement of the dopant concentration. The in situ visible–IR absorption studies[29] when combined with electrochemical voltage spectroscopy (EVS) demonstrate[30] that the charge is stored in the mid-gap states. Moreover, the EVS data give directly the energies for charge injection and removal.[30] The results[29] of in situ measurements (performed during electrochemical doping) of the visible–IR absorption in *trans*-$(CH)_x$ are shown in Figure 5. As the doping proceeds, the mid-gap absorption appears, centered near 0.65–0.75 eV, with an intensity that increases monotonically in proportion to the dopant concentration.

The mid-gap optical absorption provides direct evidence for charged soliton states in doped polyacetylene. Independent evidence has been obtained from the doping-induced modes[31,32] that appear in the mid-infrared associated with the local vibrational modes of the charged bond-alternation domain wall. Again, these mid-infrared modes are independent of dopant[2b] and show characteristic shifts after deuteriation,[32] i.e., for $(CD)_x$ compared with $(CH)_x$. That all of these spectroscopic features are associated with charged solitons has been proved unambiguously through a series of photoinduced absorption[33–35] and photoinduced ESR measurements.[36]

The remarkable oscillator strength associated with these doping-induced spectroscopic features arises directly from the spatial extent of the charge-storage state.[37] Whereas one might anticipate that the ratio of oscillator strengths would be equal to the dopant concentration, a detailed theoretical analysis shows that for dilute concentrations the mid-gap transition is enhanced by a factor of about $2l$, where $2l$ is the full width of the bond-alternation domain wall and a is the carbon–carbon spacing along the $(CH)_x$ chain. Because $2l \approx 14$, this enhancement of the soliton transition makes it observable even at highly dilute dopant concentrations.

B. Polypyrrole

Pyrrole is known to polymerize to give black conducting powder referred to as "pyrrole black".[38] In its doped form, polypyrrole (PP) has better chemical and thermal stability than Shirakawa-polymerized poly-

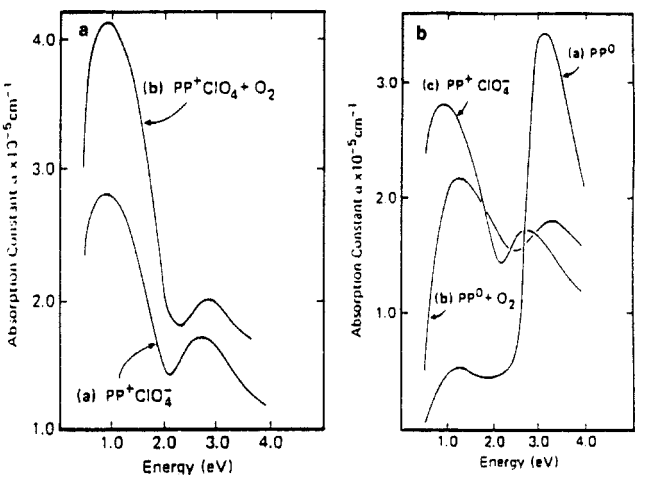

Figure 6. (a) Optical absorption curves of polypyrrole (a) before and (b) after exposure to oxygen. (b) Optical absorption curves for (a) neutral polypyrrole before exposure to oxygen, (b) neutral polypyrrole after exposure to oxygen, and (c) polypyrrole perchlorate.

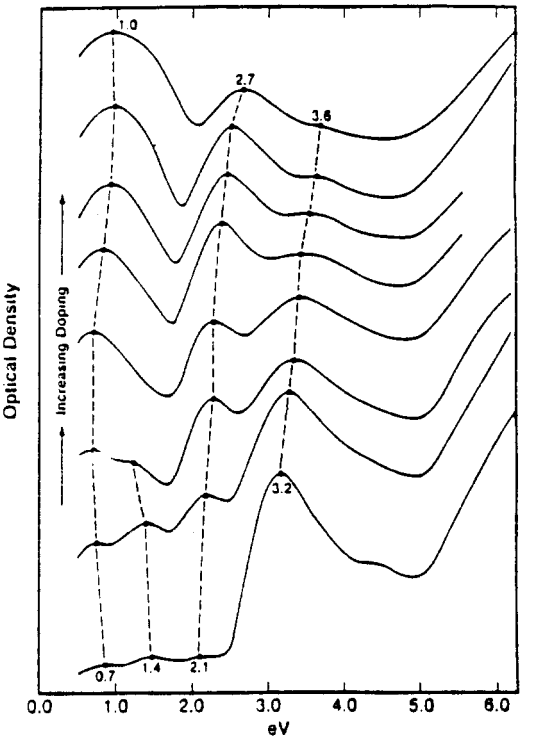

Figure 7. Optical absorption spectra of ClO_4^--doped polypyrrole as a function of dopant concentration. The dopant level increases from the bottom curve (almost neutral polypyrrole) to the top curve (33 mol % doping level).

acetylene. It has been shown by CPMAS ^{13}C NMR and IR techniques that polymerization occurs mainly by α-substitution.[39] The polymerization of the pyrrole can be carried out chemically or electrochemically. Chemical polymerization can be carried out both in solution and from the gas phase to give black conducting powder.

In the neutral form, polypyrrole films are yellow/green and are sensitive to air and oxygen. The electrochemically freshly prepared films are in their oxidized form and are copper–bronze when viewed in reflection. The effect of oxygen on the neutral film of polypyrrole was studied by Street et al.[39] The data in Figure 6 were obtained for pyrrole film samples electrochemically deposited on a nesa glass microscopic slide. The absorption data for the gray transparent oxidized polypyrrole perchlorate film before exposure to oxygen is shown in Figure 6. These absorption data for oxidized films are similar to those reported previously by Kanazawa et al.[22] These authors interpreted the broad band peak near 1.0 eV as due to the conduction electrons. The peak near 3.0 eV was associated with an interband transition derived from the $\pi-\pi^*$ transition of the pyrrole moiety.[40] On exposure of the gray film of oxidized pyrrole to 330 Torr of dry oxygen, the intensity of the ~1.0-eV "free carrier" peak increases significantly (Figure 6a). After several hours of pumping at 10^{-6} Torr, the ~1.0-eV peak decreased to $\alpha \sim 3.5$ cm^{-1}.

The absorption spectrum of the yellow/green neutral polypyrrole before exposure to oxygen (Figure 6) shows two peaks: a major one at ~3.2 eV and a smaller peak near 1.3 eV. The yellow/green film of neutral polypyrrole rapidly becomes black on exposure to oxygen and the ~3.2-eV peak height decreases by a factor of 2; the low-energy 1.3-eV peak increases until it becomes the dominant peak. The general appearance of the spectrum of this film is very similar to that of electrochemically oxidized pyrrole (Figure 6), though there are some small shifts in the energy of the two peaks. It is interesting to note that for both PP^+ and PP^0, reaction with oxygen leads to an increase in the intensities of peaks associated with the free carriers in the 1-eV region. This increase in intensity is accompanied by an increase in the conductivity of the neutral polymer from $<10^{-5}$ to 10^{-2} S cm^{-1}; however, the conductivity of the PP^+ does not increase. This was interpreted as the ~1.0-eV peak not being directly associated with free carriers. This peak is therefore probably not intrinsic to the neutral polymer but reflects partial oxidation.

The optical properties of polypyrrole perchlorate at intermediate stages of oxidation between the conducting and insulating forms were studied by Yakushi et al.[41] Polypyrrole perchlorate films for optical studies were prepared by electrochemical polymerization in a glovebox using Pt as electrode and tetrabutylammonium perchlorate as electrolyte in dry deoxygenated acetonitrile solution. The films at various stages of reduction were prepared by controlling the potential during the electrochemical reduction of as-grown polypyrrole perchlorate film in acetonitrile solution of tetrabutylammonium perchlorate. The reduction was achieved by holding the films at a fixed potential maintained for approximately 30 min, during which time the reducing current fell to zero.

Figure 7 shows the absorption spectrum of "as-grown" polypyrrole perchlorate film together with the spectra of a series of such films subjected to various reduction potentials.[41] The voltages shown in Figure 7 were those applied between the working and counter electrodes, which were separated by 6 mm. The optical densities of the films in Figure 7 are not strictly comparable because each spectrum was measured by using a different free-standing film, the thickness of which varied by ~15%.

The as-grown films of polypyrrole perchlorate have absorption bands at 1.0 and 2.7 eV and a weak shoulder at ~3.6 eV. The most strongly reduced films have a

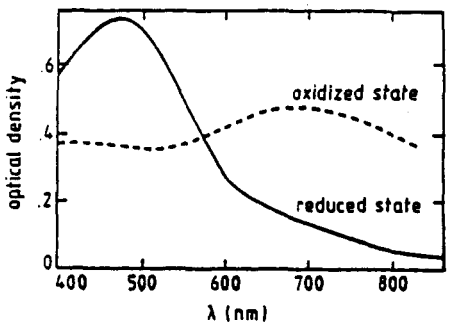

Figure 8. Visible absorption spectra of films of poly(2,2′-bithiophene) deposited on conducting glasses (thickness, 0.1 μm).

strong absorption band at 3.2 eV, a shoulder at 4.5 eV, and three very weak absorption bands at 0.7, 1.4, and 2.1 eV. As the extent of reduction increases, the intensities of the 1.0- and 2.7-eV bands characteristic of the as-grown film decrease and shift to the red. At the same time the shoulder at 3.6 eV increases and also shifts to the red.

The 3.2-eV band in the reduced form has been assigned to the π–π^* transition of the π electrons in the highest occupied molecular orbital. Initially Yakushi et al.[41] interpreted the data in terms of the presence of a range of conjugation lengths in polypyrrole films. The red shift in the 2.7-eV peak upon reduction of the film to the neutral state was interpreted as being due to a more facile reduction of conjugated segments compared to longer conjugated segments. The 2.1-eV peak in the reduced film was assigned to residual oxidized long conjugated segment. The data have been, however, recently interpreted as evidence for the presence of polarons and bipolarons in polypyrrole.[2c]

The PP absorptions below the gap at 0.7, 1.4, and 2.1 eV of polypyrrole have been attributed to the presence of polarons. At an intermediate doping level, the absorption at 1.4 eV disappears. This absorption was also observed to disappear at low doping level during a study of its evolution as a function of time.[42] ESR measurements have shown a correlation between the appearance of additional spins and the presence of the 1.4-eV peak,[42] which suggests that the 1.4-eV peak is related to polarons (radical cations) that eventually recombine into thermodynamically more stable bipolarons (dications). At an intermediate doping level, the two wide optical absorptions peaking at 1.0 and 2.7 eV are in agreement with the existence of two bipolaron bands. The band gap transition shift to higher energies, 3.6 eV, is also in agreement with the calculated value by Brêdas et al.[43,44]

C. Polythiophene

Polythiophene (PT) and its derivatives are the first examples of conducting polymers that are stable toward oxygen and moisture both in their undoped and in their doped states. They can be synthesized chemically or electrochemically. A chemically synthesized polymer is produced in its undoped insulating state and can be doped chemically or electrochemically to its conducting state. The electrochemically synthesized polymer is, however, obtained in the oxidized (doped) conducting state and can be "chemically" compensated (NH_3, hydrazine, etc.) or electrochemically "undoped" to its insulating state. Garnier et al. have studied the absorption spectra of doped and undoped polythiophene, poly(2,2′-bithiophene), and poly(3-methylthiophene).[45] Figure 8 shows visible absorption spectra of the oxidized and reduced state of poly(2,2′-bithiophene) deposited on conducting glass. The neutral ("doped") polymer has a strong absorption band at 480 nm characteristic of the π–π^* interband transition. On doping, the interband transition decreases and the absorption peak shifts toward higher energy. In an electrochemical cell, the conductivity of these systems can be switched between the conducting and insulating states by application of the appropriate voltage. Since this switching is accompanied by a color change, these materials have potential electrochromic display applications.

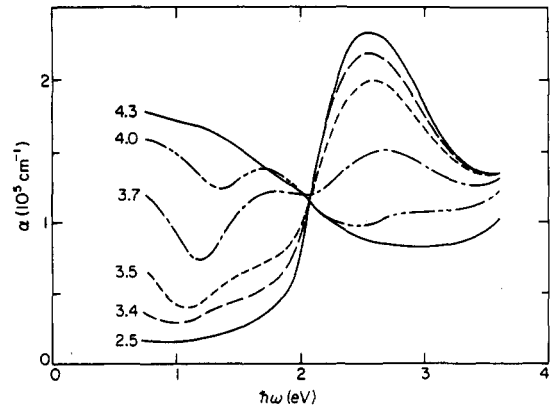

Figure 9. In situ absorption curves for polythiophene during electrochemical doping with ClO_4^-. The applied voltages (against Li) are shown on the left. The corresponding concentrations were obtained as EVS measurements and are as follows (in mol % per thiophene ring): 3.60 V (y = 2.8%); 3.65 V (y = 4%); 3.70 V (y = 5.4%); 3.80 V (y = 9.6%); 3.85 V (y = 12%); 3.90 V (y = 14%); 4.05 V (y = 20%).

Chung et al.[25] have studied in detail the in situ absorption spectroscopy during electrochemical doping. The PT sample used for the optical study was prepared by electrochemical polymerization using bithiophene as a monomer. The polymerization was done under mild conditions (low voltage, ~3.8 V vs Li; current density, 0.5 mA cm^{-2}) and the sample film was obtained on ITO glass using Al as a cathode and $LiClO_4$ as electrolyte solution.

Figure 9 shows a series of spectra[25] taken in situ during the doping cycle as the doping proceeded via the oxidation reaction shown in eq I.

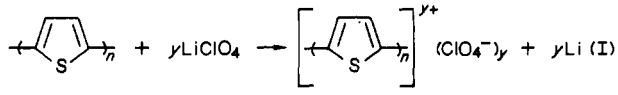

The different applied voltages correspond to different doping levels (y): 3.5 V (y = 2.8%); 3.65 V (y = 4%); 3.7 V (y = 5.4%); 3.8 V (y = 9.6%); 3.85 V (y = 12%); 3.9 V (y = 14%); 4.05 V (y = 20%). In each case the cell was allowed to reach quasi-equilibrium before the spectra were taken. Doping levels (y) were obtained from direct electrochemical measurements for V_{app} against Q in a parallel experiment using electrochemical voltage spectroscopy.[25] As the doping level increased, the intensity of the interband transition decreased continuously and the absorption peak shifted toward higher energy. In addition, two new absorption features appeared in the IR below the gap edge with intensities

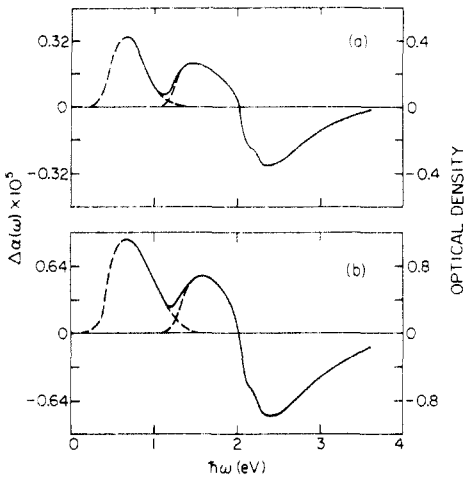

Figure 10. Difference spectra obtained from the data of Figure 9: (a) V_{app} = 3.65 V, y = 4% (or 1% per carbon); (b) V_{app} = 3.85 V, y = 12% (or 3% per carbon). In each case, the neutral-point spectrum (V_{app} = 2.50 V) was used as the reference. The broken curves are extrapolation that attempt to separate the contributions from the two absorption peaks.

that increased as the dopant level increased. The lower energy IR peak remains at a constant energy (ca. 0.65 eV) while the higher energy peak shifts toward higher energy as the dopant level is increased. At an applied doping potential of 4.3 V, the frequency-dependent absorption is characteristic of the free carrier spectrum of the metallic state, similar to that found in heavily doped (either chemically or electrochemically) polyacetylene.[2b]

The spectra of Figure 9 for $\hbar\omega > 0.8$ eV were obtained by using an identical cell (but with no sample) as reference. However, below 0.8 eV the strong absorption of the electrolyte solution limited the accuracy of the data. The extension of the curves on Figure 9 below 0.8 eV was performed on selected individual samples that were doped (to a particular applied voltage), washed, dried, and sealed in a tube.

Better accuracy was obtained by analyzing the difference spectra from the sample. Two examples are shown in Figure 10a (V_{app} = 3.65 V, y = 1% per carbon) and Figure 10b (3.85 V, y = 3% per carbon). In each case the spectrum was taken at the appropriate applied cell voltage (against Li) and the neutral-point spectrum (2.5 V, y = 0) was used as the reference. The two dopant-induced infrared bands are seen clearly with peaks at $\hbar\omega_1$ = 0.65 eV and $\hbar\omega_2$ = 1.5 eV. As noted above, $\hbar\omega_1$ is essentially independent of dopant concentration whereas $\hbar\omega_2$ increases with increasing frequency. Examination of Figures 9 and 10 indicates that the oscillator strength of these two dopant-induced IR absorption bands is comparable to that of the mid-gap absorption in polyacetylene, indicating that these two absorption features arise from electronic transitions between the valence band and two localized energy levels that appear in the gap upon charge-transfer doping.

The difference spectra of Figure 10 show that the oscillator strength that appears below the gap edge comes primarily from the interband transition. In contrast to *trans*-polyacetylene,[29,37] the loss of interband oscillator strength is not uniform but is greatest for frequencies near the band edge.

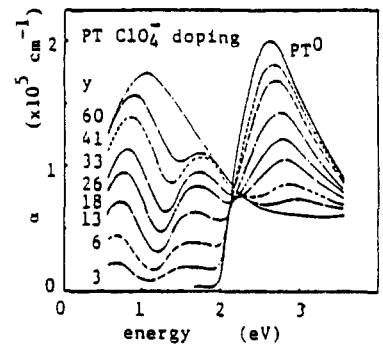

Figure 11. Absorption spectra of PT during electrochemical doping of ClO_4^-.

A procedure similar to that described above was performed in the subsequent electrochemical undoping process by using a series of stepped-down constant applied potentials. The electrochemical reaction is the reverse of eq I. At V_{app} = 2.5 V, the spectrum of undoped polythiophene was reproduced.

Both in the doping and in the undoping parts of the cycle, an isosbestic point appears at $\hbar\omega$ = 2.0 eV for dilute doping levels. At higher dopant concentrations (e.g., for $V_{app} > 3.85$ V, $y < 3\%$ per carbon) this isosbestic point disappears and the spectrum qualitatively changes, evolving toward that of the metallic limit.

Kaneto et al.[46] have studied the absorption spectra of PT film during electrochemical ClO_4^- doping. Figure 11 shows absorption spectra as a function of dopant concentration. The peaks at 0.7–0.9 and 1.5–1.8 eV show a blue shift with increasing dopant concentration and a tendency to merge into a single, broad absorption in the infrared at the highest dopant concentration. Kaneto et al. observed the formation of charge carrier with spins only below 3 mol % of dopant concentration. From the optical and ESR studies their conclusion was similar to that of Chung et al., that the charge is stored predominantly in bipolarons.[25]

D. Poly(isothianaphthene)

The spectroscopic results presented above, in combination with theoretical calculations, were used to design poly(isothianaphthene) (PITN), a polymer having the smallest energy gap of any known conjugated polymer.[47] PITN was prepared in three different ways from isothianaphthene, including electrochemical synthesis.[47a] Upon doping, the conductivity of PITN increases several orders of magnitude up to about 50 S cm^{-1}. Doping–undoping cycles are electrochemically reversible and are accompanied by a high-contrast electrochromic color change. In the undoped state, thin films of PITN are blue-black; upon doping, they become transparent yellow. Doped PITN is thus the first example of a transparent highly conducting organic polymer. In its highest doped state, PITN is very unstable in the atmosphere, a property unique to this heterocycle.

The absorption spectrum of PITN films was studied as a function of photon energy. Figure 12 shows the comparison of the spectrum of an as-grown film (dashed curve) with the spectrum of a film that was compensated electrochemically (Figure 12b, solid curve) and by ammonia (Figure 12a, solid curve). The spectrum

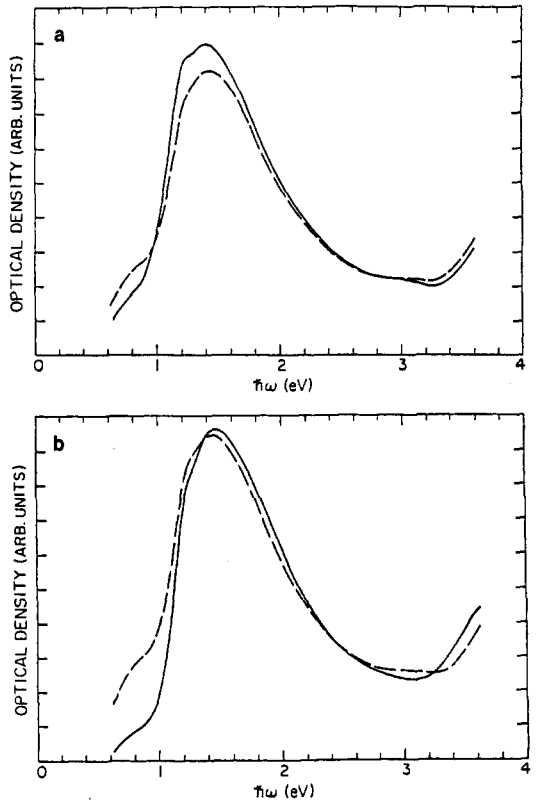

Figure 12. (a) Absorption coefficient of PITN vs photon energy. Dashed curve, as grown; solid curve, after composition with ammonia. (b) Absorption coefficient of PITN vs photon energy. Dashed curve, as grown; solid curve, after electrochemical compensation.

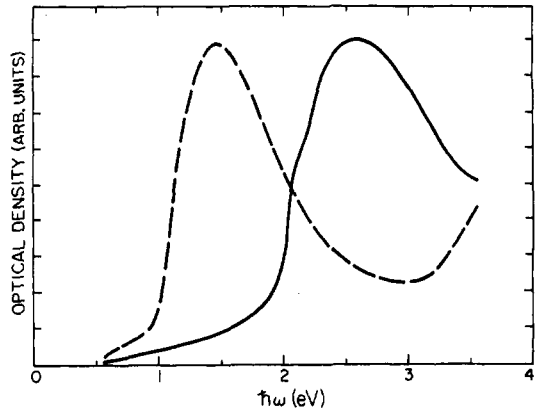

Figure 13. Absorption coefficients of polythiophene (solid curve) and poly(isothianaphthene) (dashed curve).

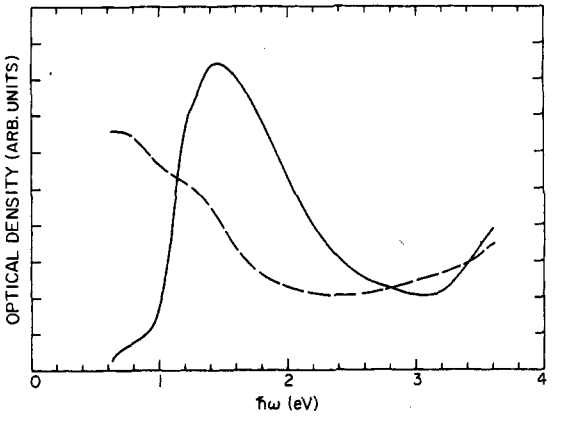

Figure 14. Spectral changes associated with the observed color change on doping; absorption spectrum of PITN after electrochemical compensation (solid curve) and after in situ electrochemical doping (dashed curve) (see text).

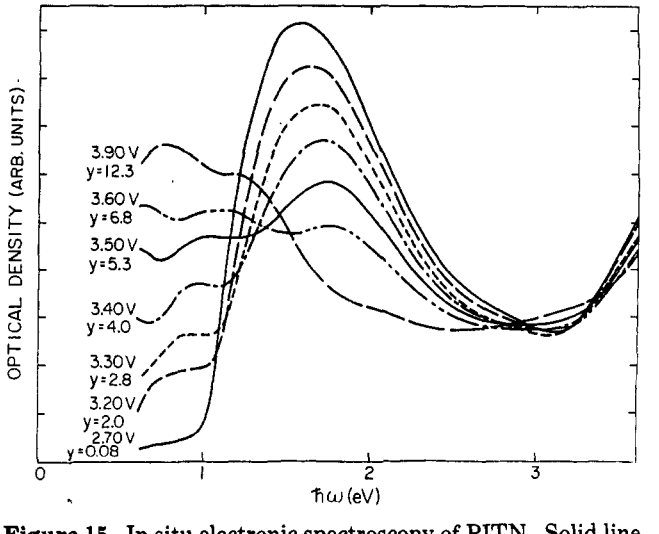

Figure 15. In situ electronic spectroscopy of PITN. Solid line at 2.7 V is a 6% Cl^--doped sample and the 3.9-V line corresponds to the same sample, fully doped. Voltages are vs Li.

consists of an intense interband absorption with a peak at $\hbar\omega \simeq 1.4$ eV, a weak shoulder on the low-energy side, and an indication of a second absorption band at higher energies ($\hbar\omega > 3.5$ eV). The weak shoulder at lower energy arises from the 5% doping of the as-grown films; the shoulder decreases in magnitude after compensation with NH_3 (dashed curve on Figure 12a). The in situ spectrum of an electrochemically compensated film (undoped electrochemically to $\simeq 2.5$ V with respect to Li) is presented in Figure 12b. There is a small blue shift (~ 0.05 eV) with the PITN sample in the electrolyte, perhaps indicative of some solvent penetration. The data of Figure 12 indicate that the low-energy shoulder is not an intrinsic feature of the neutral polymer; the onset of intrinsic absorption occurs at $\hbar\omega \simeq 1$ eV, implying that the energy gap of pure PITN is $\simeq 1$ eV. The PITN absorption (from Figure 12) is compared with the corresponding data from polythiophene in Figure 13. The similar shapes of the two curves, even including the sharp feature on the leading edge, demonstrates clearly the reduction of the energy gap of PITN to about half that of the parent polythiophene.

The spectral features associated with the observed color change on doping are shown in Figure 14, in which the absorption spectrum of electrochemically compensated PITN is compared with that obtained after electrochemical doping (p type with ClO_4^-). These data were obtained in situ with the thin film sample on conducting glass in a sealed electrochemical cell (~ 0.2 m $LiClO_4$ in propylene carbonate electrolyte with the PITN sample at the neutral point, ~ 2.4 V vs Li); the dashed curve corresponds to the maximum doping level for which the cell was stable, ~ 4.3 V vs Li. In situ measurements of the visible–IR absorption spectrum as a function of dopant concentration provide information on the changes in electronic structure that occur during doping. Absorption data for a series of applied voltage vs Li are given in Figure 15. For this study,

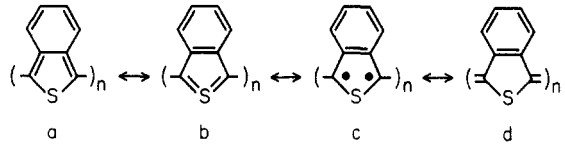

Figure 16. The various resonance contributors for PITN.

the sample was mounted in a cell similar to that used by Chung et al. in their study of polythiophene.[25] The working electrode was the polymer on ITO glass and the counter electrode was lithium metal scraped clean of its oxide layer and pressed into nickel mesh under an argon atmosphere. The cell was constructed in a controlled-atmosphere drybox.

After doping, there is no indication of an energy gap over the limited spectral range, suggesting that the electronic structure of heavily doped PITN is that of a metal and the spectral changes shown in Figures 14 and 15 are qualitatively similar to those obtained for polythiophene[25] and polyacetylene[48] where a variety of related experiments have confirmed the existence of a metallic state at high doping levels.[2b,49]

The spectroscopic data demonstrate that PITN is a small band gap semiconductor with $E_g \sim 1$ eV. The overall shape of the interband transition is remarkably similar to that reported for polythiophene and polyacetylene. The major reduction of the energy gap compared with that of the parent polythiophene presumably results from a combination of effects: namely (i) the many resonance contributors shown in Figure 16 would be expected to lead to higher stability and more nearly equal bond lengths along the pseudo-polyene backbone; (ii) the polarizability of the benzene ring would tend to reduce the repulsive electron–electron interactions between two π electrons on the same monomer unit or on neighboring carbons along the backbone.

The small band gap is consistent with the quantum chemical calculations of Brēdas et al.,[47d] who find that for conjugated polymers based on aromatic rings the band gap decreases as the quinoid character of the backbone increases. For PITN, the benzene ring built onto the thiophene monomer forces some quinoidal contribution into the ground state of the five-membered sulfur-containing ring and thereby leads to a reduction of the energy gap.

E. Poly(alkylthiophenes)

To be potentially useful in electronic applications, a material must be environmentally stable, have excellent electronic and mechanical properties, and be solution or melt processible. The delocalized electronic structures of π-conjugated polymers which are responsible for their unusual electronic properties tend to yield relatively stiff chains with little flexibility and with relatively strong interchain attractive interaction which make them insoluble and nonprocessible.

Formmer et al.[50] successfully made solutions of conducting polymers by performing the doping in the presence of a specific solvent that allowed the polymer to dissolve as it was doped. They dissolved poly(phenylene sulfide) (PPS) powder in AsF_3 solvent while at the same time oxidizing with AsF_5. This resulted in a

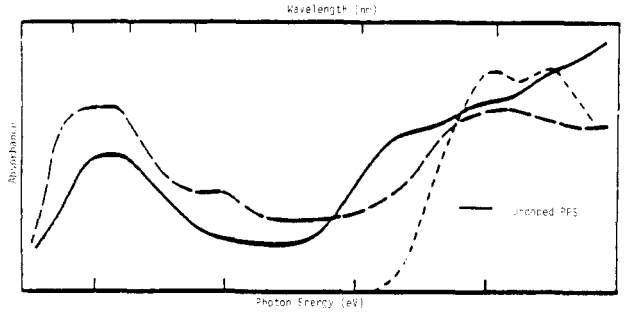

Figure 17. Optical absorption of PPS. Solid line, melt-molded film (~0.5 mm thick) doped with AsF_5; dashed line, AsF_5 doped in AsF_3 solution, ~0.01 m in monomer repeat units (–S–Ph–).

blue conducting polymer solution from which conducting films could be cast on different substrates. These films exhibited conductivities from 25 to 200 S cm^{-1}. The high conductivities in these samples cast from solution were speculated to arise from the homogeneous distribution of dopant throughout the polymer film.

Electronic absorption spectra of both solution and films of doped PPS have been recorded in the visible–IR region[50] (Figure 17). The basic similarities between optical spectra obtained on conventionally doped PPS solid and on doped PPS solutions indicate that the AsF_3–AsF_5 solution is a conducting polymer solution.

Jenekhe et al.[51] reported another processible polymer in liquid I_2 from which also a conducting film could be cast. Although this work represents important progress, toxicity and environmental instability of these solvent systems (AsF_3–AsF_5 or liquid I_2) make them undesirable.

Recently, several groups have prepared soluble, highly conducting, and environmentally stable polythiophenes having long alkyl chains.[52–54] In these polymers, solubility can be achieved through addition of an appropriate side group. Thus, whereas neither PT nor poly(3-methylthiophene) (P3MT) is soluble, the addition of relatively long, flexible, hydrocarbon chains to the thiophene ring has increased the solubility and processibility of this conjugated polyheterocycle without significantly changing the π-electronic structure. Since these polythiophene derivatives are soluble in common organic solvents (chloroform, THF, etc.) in both their neutral and conductive (doped) forms, they have opened the way to study optical and magnetic properties in solution as well as charge-storage configurations of doped isolated macromolecules in dilute solution.

Several soluble polythiophenes have been synthesized by electrochemical polymerization of thiophene derivatives having a flexible side chain at the 3-position. Polymers studied were poly(3-hexylthiophene) (P3HT), poly(3-octylthiophene) (P3OT), poly(3-dodecylthiophene) (P3DDT), poly(3-octadecylthiophene) (P3ODT), and poly(3-icosylthiophene) (P3IT). The conductivities of oxidized films of P3HT, P3OT, P3DDT, P3ODT, and P3IT were 10–100 S/cm. The IR spectra of solution-cast films were the same as those of neutral films obtained by electrochemical reduction of as-grown films, indicating that no deterioration took place during dissolving, casting, and drying.[52–54]

The existence of π-conjugation in these materials is implied by their colors and their electronic spectra. The

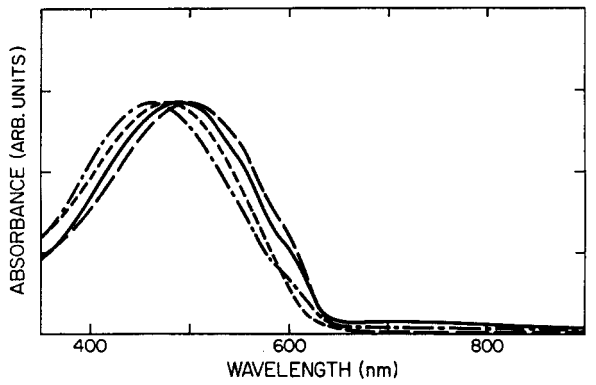

Figure 18. Absorption spectra of PT and a few alkyl derivatives of 3-substituted PTs: (---) PT; (– – –) P3MT; (····) P3BT; (—) P3HT.

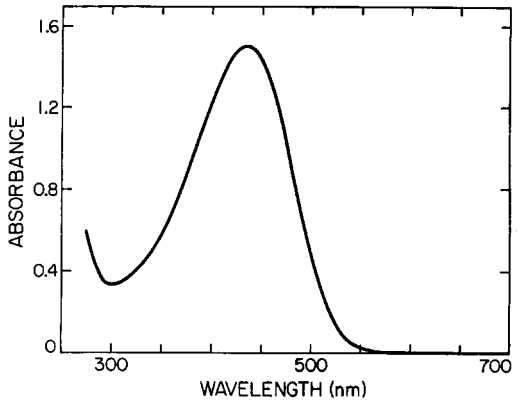

Figure 19. Absorption spectrum of P3HT/THF solution (≈2 × 10^{-4} M) at room temperature.

electronic absorption spectra of the P3ATs (Figure 18) indicate that the band edge occurs at about 2 eV, a value that is typical for the entire P3AT series. Although slight shifts in the edge and in the weak shoulder just above the edge are observed, the data are essentially independent of the alkyl substituent.

Figure 19 shows the UV–visible absorption spectrum of a P3HT/THF solution. The maximum extinction coefficient (at 435 nm) is approximately 8800 mL^{-1} cm^{-1}. On dissolution, a major shift of the π–π^* absorption band is observed (Figures 18 and 19).

The absorption spectra of P3HT for as-synthesized and solution-cast films are compared in Figure 20[54] (the corresponding spectra for the P3BT are essentially the same as those of P3HT). The spectral characteristics of the solution-cast films are nearly identical with those of the as-synthesized films both in the neutral case and after doping (with ClO_4^- ions). It is noteworthy that the π–π^* absorption edge is neither shifted nor significantly broadened. In addition, the residual absorption below the interband transition is extremely weak for the solution-cast films, indicating the absence of impurity or disorder-induced states in the gap.

Both as-synthesized and solution-cast films can be readily doped with resulting electrical conductivities that are quite high; e.g., $\sigma \approx 40$ S cm^{-1} for films of poly(butylthienylene). UV–visible absorption spectra of these soluble polythienylenes have been obtained for solid films (as synthesized and solution cast) and for the polymers in solution. The spectral characteristics of the solution-cast films are essentially identical with those of the as-synthesized films both in the neutral

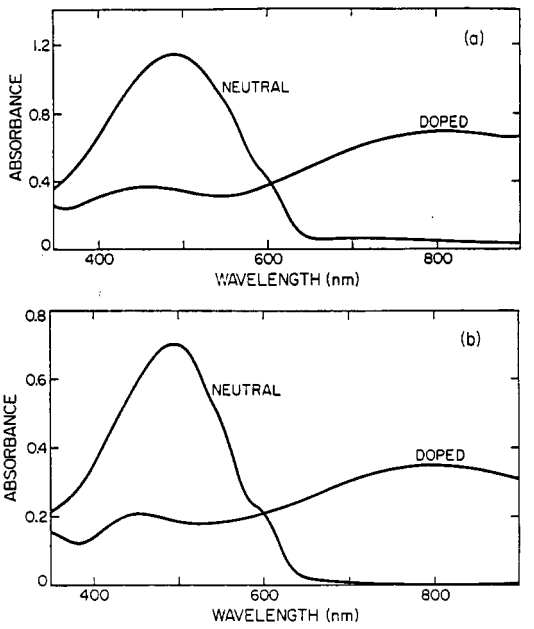

Figure 20. Absorption spectra of neutral (undoped) and conducting (doped) P3HT films at room temperature: (a) as-synthesized film; (b) solution-cast film.

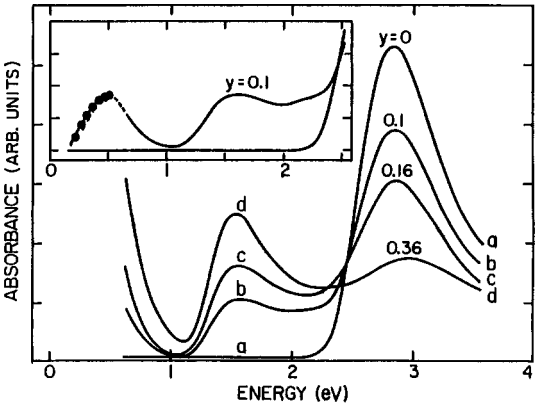

Figure 21. Absorption spectra of the neutral and doped polymer ($y \approx 0.1$, 0.16, and 0.36) at a P3HT concentration of $C_0/100$ (in chloroform). The inset shows an extended-range IR spectrum (obtained with $C \approx C_0$ in chloroform).

state and after doping. The comparison of the spectra of the as-grown and solution-cast films suggests that the electronic structure of the P3ATs is unchanged after dissolution and subsequent processing into thin solid films, and the solution-cast films have a well-defined electronic structure that is equivalent in overall features to that of the most highly crystalline polythiophene (in fact, the absorption edge is even sharper and the residual absorption below the edge is even weaker than observed for chemically coupled, annealed polythiophene). This implies weak interchain electronic interactions; i.e., the electronic structure is highly anisotropic or quasi-one-dimensional. This quasi-one-dimensionality is consistent with the good solubility of the alkyl-substituted polymer. The combination of high conductivity and weak interchain coupling implies that electronic motion along the conjugated chains is the dominant transport mechanism.

The absorption spectra of the neutral and the doped polymer at different doping ($y \approx 0.1$, 0.16, and 0.36) are compared in Figure 21 for a polymer concentration of $C_0/100$ (C_0 = 1 mg/mL, 6 × 10^{-3} m).[54] The effect of

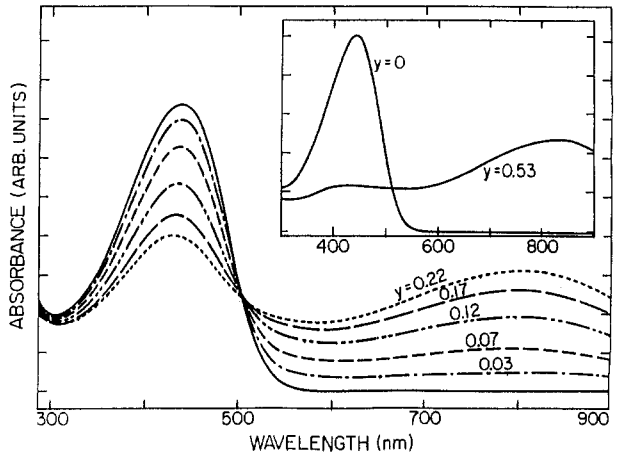

Figure 22. Series of visible–near-IR absorption spectra taken at successively higher doping levels (P3HT concentration $0.4C_0$ in chloroform). The inset compares the spectra for the neutral polymer solution with that for maximum doping ($y \approx 0.53$) at $C \approx C_0/100$.

doping is characteristic of conducting polymers. The π–π^* transition is depleted with the oscillator strength shifted onto two principal subgap features in the infrared. That the low-energy feature is indeed a peak (implying two localized gap states) is demonstrated in the inset, where the broad-band mid-IR absorption and the near-IR spectrum (obtained with two different instruments) are superposed. The data in the inset were obtained at a polymer concentration of $C \approx C_0$. Additional weak absorption can be seen in the inset $\hbar\omega \approx 2.15$ eV; excess absorption is also observed at this energy in the spectrum taken with $C_0/100$ (C_0 = 1 mg/mL); this feature shows up clearly in difference spectra. The two principal subgap absorption bands with maxima at $\hbar\omega_1 \approx 1.55$ eV and $\hbar\omega_2 \approx 0.5$ eV in the doped polymer are consistent with charge storage predominantly in bipolarons. The π–π^* transition energy (onset at ≈2.2 eV, peak at ≈2.8 eV) is, however, greater than $(\hbar\omega_1 + \hbar\omega_2) \approx 2.05$ eV.

The additional absorption near 2.15 eV is not the result of a (third) polaron mode. Detailed examination of difference spectra shows that this feature decreases in relative high strength at high y and at high C, whereas the magnetic data indicate in both cases a monotonic increase in the number of polarons per ring.

A series of visible–near-IR spectra taken at successively higher doping levels (polymer concentration of 0.4 mg/mL) are shown in Figure 22. The well-defined isosbestic point at 505 nm (2.45 eV) implies the coexistence (and interconversion) of two regions on a doped P3HT chain, neutral regions where the π–π^* transition is unchanged and localized regions surrounding the charge-storage configuration (bipolarons). As the doping level is increased, the subgap absorption grows at the expense of the π–π^* transition; at high doping levels in dilute solution (see inset to Figure 22), nearly all the π-electron oscillator strength has been shifted into the two intense infrared bands.

The magnetic resonance data demonstrate that at dilute concentrations (i.e., in the isolated single-chain limit) charge is stored predominantly in a spinless configuration for doped P3HT in solution. For dilute solutions ($C \ll C_0$), virtually all the charge is stored in bipolarons; polarons are formed only as a result of an odd number of charges on a single macromolecule.

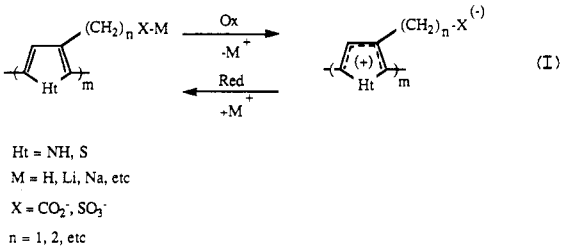

Figure 23. Self-doped polymers.

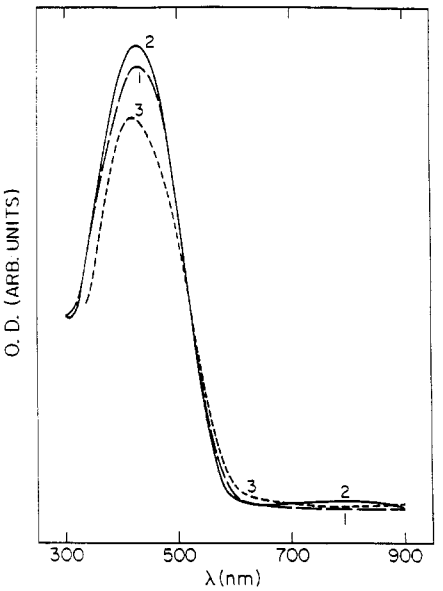

Figure 24. Electronic (UV–visible) absorption spectra of cast films of P3-ETSNa (curve 1), of P3-ETSH (curve 2), and of the methyl ester of P3-ETS (curve 3).

F. Poly(thiophenealkanesulfonates): Self-Doped Polymers That Are Water Soluble

Recently, the sodium salts and the "proton salts" (acids) of poly(3-thiopheneethanesulfonate) (P3-ETSNa and P3-ETSH, respectively) and poly(3-thiophenebutanesulfonate) (P3-BTSNa and P3-BTSH, respectively) were prepared.[55,56] In these polymers, the counterions are covalently bound to the polymer backbone, leading to the self-doped concept. In the self-doped conjugated polymer, charge injected into the π-electron system is compensated by proton (or Li^+, Na^+, etc.) ejection, leaving behind the oppositely charged counterion. The principle as applied to polyheterocycles is depicted in eq I (Figure 23).

Equation I takes the advantage of the addition of a flexible side chain in a thiophene unit like those of long-chain poly(alkylthiophenes) which make them soluble. More importantly, *these polymers are water soluble*; the class of self-doped polymers therefore contains the first known water-soluble conducting polymers.

The absorption spectra for the neutral polymer films and polymer solution in water were studied. The existence of π conjugation in these polymers is implied by their colors and their electronic spectra. The electronic (UV–visible) absorption spectra of cast films of the methyl ester of P3-ETS, of P3-ETSNa, and of P3-ETSH are shown in Figure 24. The spectra of the three polymers are virtually identical; the onset of π–π^* absorption occurs at about 600 nm (1.96 eV) and the peak

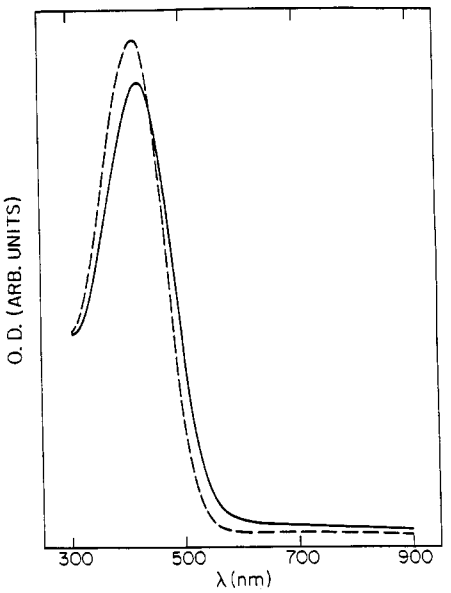

Figure 25. UV–visible spectra of P3-ETSNa (dashed line) and of P3-ETSH (solid line) in aqueous solution.

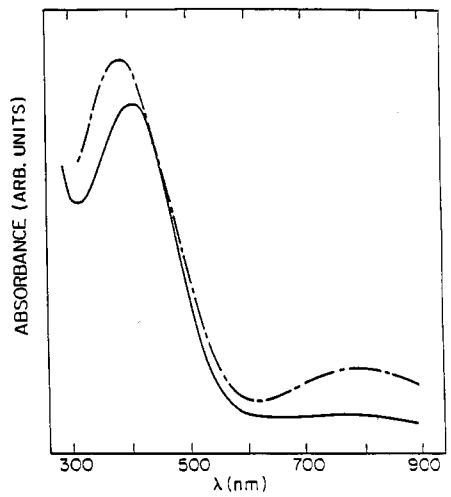

Figure 26. Comparison of the π–π^* absorption for a film of P3-BTSH (cast from water; broken curve) and for a solution of a the same polymer in water (solid curve).

is at about 425 nm ($\simeq$2.6 eV). The addition of the side chain and sulfonate group, etc., does not cause any significant changes in the electronic structure of the conjugated backbone.

Figure 25 shows UV–visible spectra of the sodium salt (P3-ETSNa) and of the acid (P3-ETSH) in aqueous solution. Both spectra are essentially identical (the absorption edge is slightly broader for the acid). The spectra of Figure 24 and 25 indicate a relatively small spectral shift upon dissolution; the onset of absorption shifts from 600 nm in the cast solid film to 550–575 nm in solution, whereas the absorption maxima are at 425 nm in both cases. This is in contrast to the results obtained from the poly(3-alkylthienylenes) where a significant blue shift is found between the solid film and the solution spectra. In Figure 26, the absorption spectra show a comparison of the π–π^* transition for a film of P3-BTSH (cast from water) and for a solution of the same polymer in water. The data once again indicate a relatively small spectral shift upon dissolution.

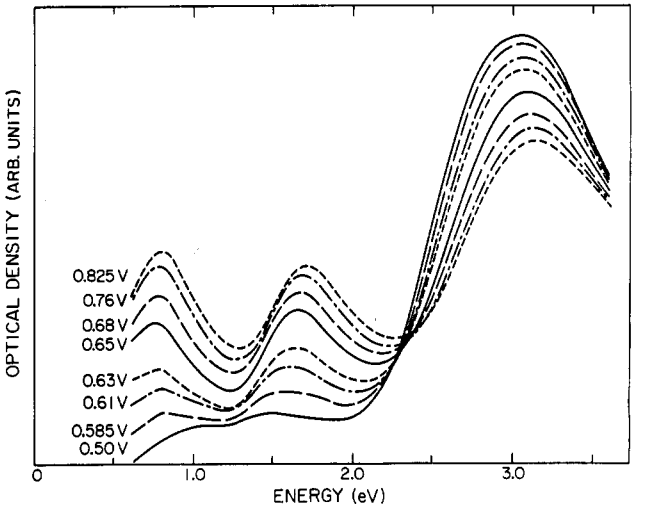

Figure 27. A series of spectra obtained from P3-ETSNa taken at different cell voltages in the relatively dilute opening region; the cells consisted of a polymer solution film cast onto a transparent indium/tin oxide (ITO) glass electrode (anode), platinum counter electrode (cathode), and a Ag/Ag^+ reference electrode in acetonitrile with tetrabutylammonium perchlorate as electrolyte.

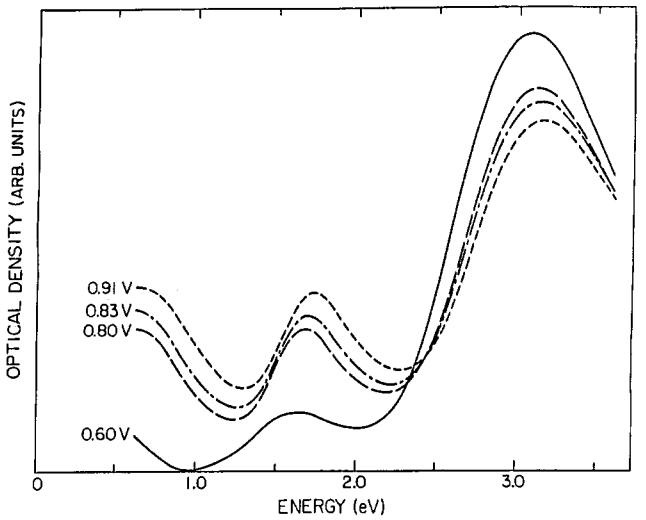

Figure 28. In situ absorption spectra of P3-ETSH; the electrolyte was fluoroboric acid–trifluoroacetic acid (at a 3:10 ratio) at a concentration of about 0.2 M in acetonitrile. The series of spectra were taken with the cell charged to successively higher open-circuit voltages. In this case, the polymer was observed to spontaneously dope in the strongly acidic electrolyte solution.

The π-electron structure of these water-soluble polythiophene derivatives is the same as that of the parent polymers, as shown by the spectra of the neutral polymers (i.e., addition of the saturated side chains has little effect on the delocalized π-electronic system). The π–π^* transition onsets near 2 eV with a peak at about 3 eV. The onset compares favorably with polythiophene; the peak is somewhat blue-shifted with respect to polythiophene. This broadening of the leading edge implies a relatively high degree of polydispersity.

The data shown in Figures 27 and 28 are consistent with charge storage as bipolarons. In each case, the following characteristic features are observed: two doping-induced transitions in the infrared, indicating the formation of two localized states in the gap. Preliminary results of in situ electron spin resonance experiments are consistent with charge storage via spinless carriers.

The experimental conditions for in situ optoelectrochemical spectroscopy were essentially those reported for the above in situ spectroscopic studies. Figure 27 shows a series of spectra obtained from P3-ETSNa taken at different cell voltages in the relatively dilute doping regime. The results are typical of polythiophene and the P3AT derivatives; the $\pi-\pi^*$ transition is depleted with a concomitant shift of oscillator strength into the two infrared bands characteristic of bipolaron formation. The same qualitative features are observed for P3-BTSNa, although the two bands are slightly shifted (by about 1.0 eV) more deeply into the infrared. We note, however, that doping occurs to a much lower extent than in all cases described above.

Spectra of P3-ETSH are shown in Figure 28. In this case, the electrolyte was fluoroboric acid–trifluoroacetic acid (in a 3:10 ratio) at a concentration of about 0.2 M in acetonitrile. The series of spectra were taken with the cell charged to successively higher open-circuit voltages. In this case, the polymer was observed to spontaneously dope in the strongly acidic electrolyte solution. The change in chemical potential of the polymer as a result of this spontaneous doping leads to the increased cell voltages noted on the figure. The appearance of two gap states is consistent with bipolaron formation. Once again, in this case complete doping was not achieved. Control of the doping level (with associated changes in the intensities of the $\pi-\pi^*$ and gap state transitions) was achieved by imposing a voltage lower than the equilibrium open-circuit voltage. This was confirmed with electrochemical measurements. The cyclic voltammetry carried out on films of the above polymer (P3-ETSH/ITO glass working electrode, platinum counter electrode, and Ag/Ag^+ reference electrode in acetonitrile with fluoroboric acid–trifluoroacetic acid as electrolyte) indicated an electrochemically robust polymer when cycled between +0.1 and +1.2 V vs Ag/Ag^+ in a strongly acid medium. The polymer could be cycled and corresponding color changes from orange to blue-green and vice versa could be observed without noticeable change in stability at 100 mV/s.

IV. Charge Storage: Solitons, Polarons, and Bipolarons

In traditional three-dimensional semiconductors, the fourfold (or sixfold, etc.) coordination of each atom to its neighbor through covalent bonds leads to a rigid structure. In such systems, therefore, the electronic excitations can usually be considered in the context of this rigid structure leading to the conventional concepts of electrons and holes as the dominant excitations. The situation in semiconductor polymers is quite different; the twofold coordination makes these systems generally more susceptible to structural distortion. As a result, the dominant "electronic" excitations are inherently coupled to chain distortions. Thus, quite generally, one expects that solitons, polarons, and bipolarons will be the excitations of major importance in this class of one-dimensional polymer semiconductors.

There are two general classes of structures which lead to qualitatively different electronic (spectroscopic) properties: (i) systems in which the ground state is twofold degenerate (*trans*-polyacetylene is the prototype example). In this case, solitons are the important excitations and the dominant charge-storage species; (ii) systems in which the ground-state degeneracy is lifted (the polyheterocycles are the principal examples). In this case polarons and bipolarons are the important excitations with charge storage in bipolarons.

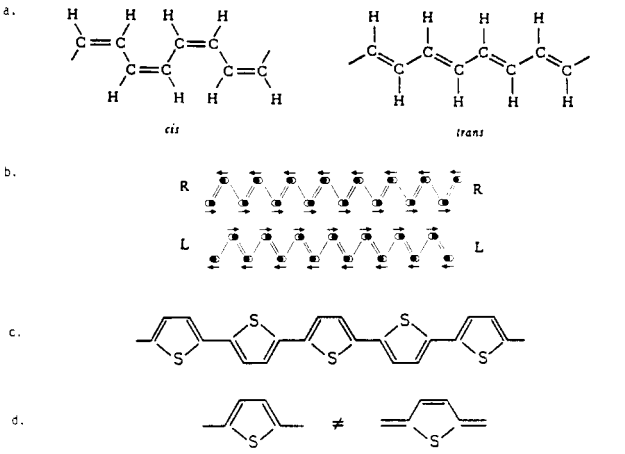

Figure 29. (a) Chemical structures of *cis*-$(CH)_x$ and *trans*-$(CH)_x$. (b) The two degenerate ground-state structures of *trans*-$(CH)_x$. The atomic distortions are indicated by the arrows. (c) Chemical structure of polythiophene. (d) Two inequivalent structures for the thiophene heterocycle in polythiophene.

As shown in Figure 29, *trans*-$(CH)_x$ is a twofold-degenerate Peierls insulator that allows for the possibility of nonlinear excitations in the form of soliton-like bond-alternation domain walls, each with an associated electronic state at the center of the energy gap.[16-18,57] For polythiophene, on the other hand, the two structures sketched in Figure 29 are not energetically equivalent. Polythiophene can be viewed as an sp^2p_z carbon chain in a structure analogous to that of *cis*-$(CH)_x$ but stabilized in that structure by the sulfur that covalently bonds to neighboring carbon atoms to form the heterocycle.

In the following section, we summarize the theoretical concepts and use them to develop a methodology for understanding the general features of the optical properties described above.

A. Solitons and Bipolarons: Some Concepts

Although single-soliton defects can exist on imperfect chains (and have been studied extensively),[58] intrinsic excitations, either photoproduced or doping-induced, must occur in the form of soliton–antisoliton ($S\bar{S}$) pairs. The energy level diagrams for neutral and positively or negatively charged solitons are shown in Figure 30. The most appropriate experimental evidence for the existence of midgap states is derived from spectroscopy (see Figure 5). This dopant-induced electronic transition has been observed to be independent of the dopant ion and of the nature of the charge (positive or negative).

Theoretical analysis[16-18,57] has demonstrated that a charged soliton represents the lowest energy configuration for an excess charge on a *trans*-$(CH)_x$ chain; i.e., $E_S < \Delta$, where E_S is the energy for creation of a soliton and Δ is the energy for creation of an electron or hole ($\Delta = E_g/2$). Both numerical calculations using a discrete lattice model and analytical results for a contin-

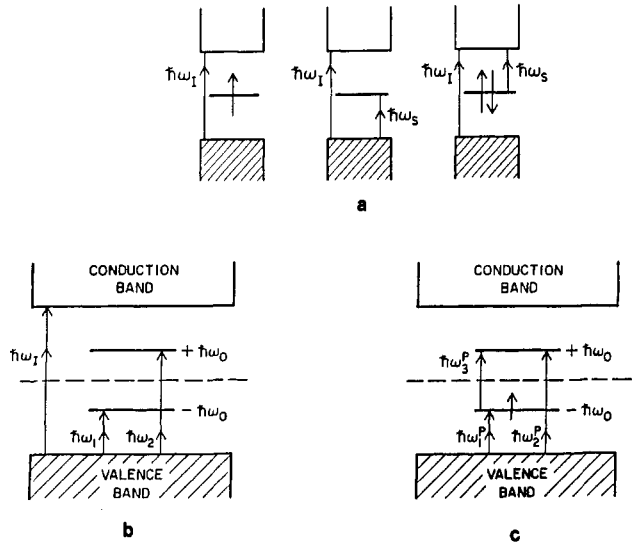

Figure 30. (a) Energy level diagram of the midgap state associated with the soliton where $\hbar\omega_I = 2\Delta$ is the interband transition and $\hbar\omega_S = \Delta$ is the midgap transition; left, neutral soliton; center, positive soliton; right, negative soliton. (b) Energy level diagram for a charged (positive) bipolaron. Because of the splitting of the levels, there are two possible transitions in addition to $\hbar\omega_I$. (c) Energy level diagram for a charged (positive) polaron. Because of the additional occupancy by the unpaired spin, there is an additional transition ($\hbar\omega_3^P$).

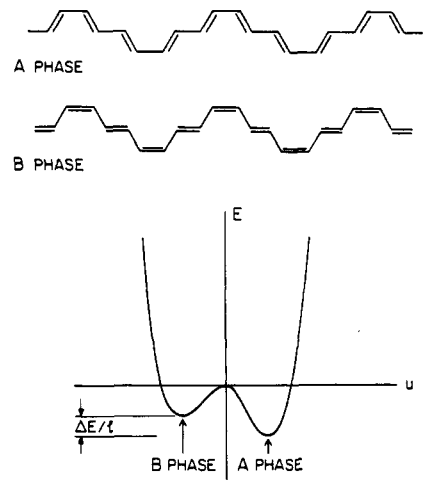

Figure 31. Schematic diagram of polythiophene backbone structure leaving out the sulfur atoms (see Figure 2). The two configurations (A phase and B phase) are nearly (but not precisely) degenerate as shown in the diagram at the bottom of the figure, where we plot energy against the distortion parameter, u (u = 0 when the bond lengths are equal).

uum model indicate that (neglecting electron–electron Coulomb interaction)

$$2E_S = (4/\pi)\Delta \qquad (1)$$

Quantum chemical calculations[43] are fully supportive of the results obtained from field theoretical models. Charged solitons are therefore formed by electron transfer onto or off the polymer chains on doping with electron donors or acceptors.

An analogy can be constructed[25] between PT and $(CH)_x$ as shown in the diagrams of Figure 31, where we redraw the polythiophene backbone structure purposely leaving out the sulfur heteroatom. The resulting structure is that of an sp^2p_z polyene chain consisting of four-carbon all-trans segments linked through a cis-like unit. Photoinduced absorption measurements[59] have demonstrated the quantitative validity of this point of view; excitations generated by optical absorption across the π–π^* energy gap interact predominantly with the pseudo-polyene backbone; the interaction with the ring modes is weak and can be ignored to first approximation. In such a structure, the ground state is not degenerate (as sketched in Figure 31). However, the energy difference per bond, $\Delta E/l$, might be expected to be small, i.e., greater than zero (as in *trans*-$(CH)_x$) but less than that of *cis*-$(CH)_x$. An obvious consequence of the lack of degeneracy is that the schematic PT structure of Figure 31 cannot support stable soliton excitations because creating a soliton pair separated by a distance d would use an energy of about $d(\Delta E/l)$. This linear "confinement" energy leads to bipolarons as the lowest energy charge-transfer configurations in such a chain with creation energy somewhat greater than $(4/\pi)\Delta$ (the creation energy for a bipolaron goes to 1 in the limit of zero confinement). The corresponding energy level diagram (for a positive bipolaron) is sketched in Figure 30b. Two gap states are for a positive bipolaron (charge 2|e|) and filled for a negative bipolaron (charge −2|e|).

1. Discussion in Terms of Confined $S\bar{S}$ Pairs, Polarons, or Bipolarons

The absorption spectrum of neutral polythiophene is remarkably similar to that of *trans*-$(CH)_x$[29,37] but blue-shifted by about 0.4–0.5 eV. Even the familar structure on the leading edge, attributed by Melé[60] to dynamical chain distortion following electron–hole creation, is evident in the data. These similarities suggest that polythiophene can be viewed as similar to *trans*-$(CH)_x$ but with the ground-state degeneracy lifted by a small amount because of the inequivalence of the two structures with opposite bond alternation. This analogy was emphasized in the schematic structure shown in Figure 29.

Although this description of PT is admittedly schematic, there is experimental evidence that it represents an excellent starting point for a more detailed description of the doping processes in this system. The optical absorption data (Figures 9 and 10) indicate an energy level structure at dilute doping levels as shown in Figure 30b with $\hbar\omega_1$ and $\hbar\omega_2$ just below the peaks because the transitions involved are between a localized gap state and the valence band density of states. The value for the interband absorption can be estimated from the data of Figures 9 and 10 to be $\hbar\omega_| \approx 2.1$ eV. In this case, the joint density of states of the valence and conduction bands is involved in the absorption so that the point of steepest slope in $\alpha(\omega)$ or the crossover in the difference curves (Figure 10) is used. Although there is surely some uncertainty in the assignment of the precise energies, the data from the dilute dopant concentrations yield

$$\hbar\omega_1 + \hbar\omega_2 \approx \hbar\omega_| = E_g \qquad (2)$$

where $E_g \equiv 2\Delta_0$ is the energy gap. The results expressed quantitatively in (2) indicate the existence of electron–hole symmetry in the doped polymer. Figure 30b shows that the two doping-induced energy levels appear symmetrically with respect to the gap center at $\pm\ \hbar\omega = 0.40 \pm 0.05$ eV. The existence of electron–hole symmetry

implies that the schematic structure of Figure 31 represents an essentially correct point of view. The sulfur atoms stabilize the polyene chain in the configuration of Figure 31 through covalent bonding to neighboring carbon atoms. However, evidently the sulfur is only weakly interacting with the π-electron system of the polyene backbone.[59] If this were not the case, some of the transferred charge would reside on the sulfur, and the electron–hole symmetry implied by Figures 9 and 10 and sketched in Figure 30b would not be present.

We assign the two energy gap states inferred from Figures 9 and 10 to the two levels expected from charge storage in bipolaron states in doped PT and the P3AT derivatives. This assignment is based on three facts:

(i) The two transitions imply formation of two levels of symmetric with respect to the gap center.

(ii) The observation of only two transitions implies that the two levels are not occupied. If there were electrons in the lower level (as there would be for a "hole" polaron), then a third absorption would be evident, arising as a transition between the two localized levels. This is not observed.

(iii) Analysis of the data leads to $\omega_0/\Delta_0 \approx 0.35$. This small value is inconsistent with polaron formation, for which $\omega_0/\Delta_0 \geq 0.797$.[18,61]

The small value inferred for ω_0/Δ_0 implies weak confinement. By using the results of Fesser[61] in their detailed analysis of the bipolaron problem, one can extract values for the relevant microscopic parameters. The confinement parameter is defined as

$$\gamma = \Delta_e/\lambda\Delta_0 \qquad (3)$$

where Δ_e is the constant external gap parameter ($2\Delta_e$ would be the energy gap without the bond alternation contribution, Δ_i, which arises from the spontaneous symmetry breaking arising from the Peierls instability), λ is the dimensionless electron–phonon coupling constant appropriate to the twofold commensurate case and Δ_0 is the the full gap parameter ($\Delta_0 = \Delta_e + \Delta_i$). From Fesser et al.[61], we obtain $\gamma \approx 0.1$–0.2 using the experimental value $\omega_0/\Delta_0 \approx 0.35$. This small value for γ, implying weak confinement, is consistent with the point of view expressed in Figure 31 and with the remarkable similarity of the shape of the absorption curves of neutral *trans*-$(CH)_x$ and neutral PT.

The one-dimensional energy gap in *trans*-$(CH)_x$ has been estimated as $E_g^{1D} \approx 1.6$–1.8 eV.[62] Taking the values of $E_g^{1D} \approx 2.1$ eV for polythiophene, one can estimate $\Delta_e \approx 0.15$–0.2 eV. Thus, from (3), one finds $\lambda \approx 0.5$–1 for PT. Although this is quite clearly not a precise determination of λ, the resulting value is reasonable. Note that even though the sulfur appears to play only a minor role in the π-electron structure of PT, the bonding to neighboring carbons to form the heterocycle may lead to significant contributions to the chain stiffness, phonon dispersion, the electron-coupling constant, etc.

The relative intensities of the two gap absorptions, $\hbar\omega_1$ and $\hbar\omega_2$, can be obtained from Figure 10. Although the in situ instrumental configuration does not allow data acquisition at frequencies below about 0.6 eV, the overall features are clear (we have sketched the extrapolated shape of $\hbar\omega$ to lower frequencies based on the line shape expected for a transition between a localized state and a one-dimensional band). The lower energy peak has the greater integrated intensity by a factor of about 2; i.e., $I(\omega_1)/I(\omega_2) \approx 2$. This ratio has been calculated by Fesser et al.,[61] who find $I(\omega_1) > I(\omega_2)$ for bipolarons, in agreement with the experimental results; however, with $\omega_0/\Delta_0 \approx 0.35$, they predict $I(\omega_1)/I(\omega_2) \approx 6$. Although the origin of this discrepancy is not clear, recent theoretical studies have shown that this ratio is sensitive to the strength of the electron–electron interactions; for intermediate coupling, the ratio is in approximate agreement with experiment. It is obvious, however, that the model is oversimplified in many ways. In the case where the ground state is degenerate, the mid-gap transitions steal oscillator strength uniformly from the interband transition. This has been observed and experimentally verified in the in situ optoelectrochemical spectroscopy studies of *trans*-$(CH)_x$.[29,37] For PT, this is not the case. Figures 9 and 10 demonstrate that as the doping proceeds the interband transition weakens, but not uniformly. The loss of oscillator strength is greater near the interband edge, causing the apparent shift to higher energies with increasing dopant concentration. Although a detailed quantitative comparison is difficult, Fesser et al.[61] have shown that the loss of oscillator strength, $\beta(\omega)$, is greater near the band edge in the case of bipolarons. By using $\omega_0/\Delta_0 \approx 0.35$ (appropriate to PT), $\beta(\omega)$ is 2 times greater for $\hbar\omega \approx E_g$ than the corresponding value at higher energies. Thus, the qualitative features of the observed changes in interband absorption are in excellent agreement with the predictions based on charge storage in bipolarons. A more detailed analysis is not possible at present because of the limited spectral range currently available.

As the dopant concentration is increased, $\hbar\omega_1$ remains essentially constant, whereas $\hbar\omega_2$ shifts toward higher energies. This concentration-dependent shift is not expected within the confines of the noninteracting bipolaron theory. The shift may signal the importance of interactions between bipolarons leading at sufficiently high concentrations to the metallic state. Alternatively, the shift may imply some involvement of the sulfur heteroatom at high dopant levels leading to a breakdown of the precise electron-hole symmetry. We note in this context that the electron spin resonance line of heavily doped metallic PT (doped with AsF_5) exhibits a small g shift (2.008) relative to that of polyacetylene under similar conditions (2.0026), implying some charge on the sulfur heteroatom at high dopant levels.[63]

In the heavily doped limit ($V_{app} = 4.3$ V), all signs of the interband transition have disappeared, and the spectrum (Figure 9) is dominated by the free carrier absorption in the infrared. In this regime, the optical properties of doped PT are those of a metal. The magnitude and spectral dependence of $\alpha(\omega)$ are similar to those reported earlier[64,65] for Na-doped *trans*-$(CH)_x$, where electrical conductivities in excess of $10^3\ \Omega^{-1}$ cm were inferred from the frequency-dependent absorption in the IR and subsequently observed directly in dc measurements.[65] Thus, metallic doped PT can be expected to be an excellent conductor. Although previous conductivity measurements on electrochemically synthesized (and doped) PT have yielded values[66] as high as 100 and 500 Ω^{-1} cm^{-1} for poly(3-methylthiophene), the intrinsic values may in fact be much higher.

Whereas charge storage in polythiophene was relatively easily interpretable in terms of bipolarons, the situation with polypyrrole is not as simple. At low doping levels, it is clear that charge is stored in the form

of polarons whose associated quinoid-like geometry relaxation extends over about four pyrrole rings. The polaron levels are about 0.5 eV away from the band edges. When a second electron is taken out of the backbone, the energetically favored species is the bipolaron which also extends over four pyrrole rings. The geometric relaxation is stronger than in the polaron case. This is reflected in the 0.75-eV energy gap between the band edges and the bipolaron states. The bipolarons' binding energy is 0.69 eV, compared to 0.12 eV for the polarons, indicating that bipolarons are favored over polarons by 0.45 eV. As shown in section III.B, this is supported by ESR measurements on oxygen-doped PP.

The overlap between bipolaron states in the gap leads to the formation of two 0.4-eV-wide bipolaron bands in the gap and at the same time the gap widens from 3.2 to 3.6 eV in the 33% doped material. This is due to the fact that the bipolaron states in the gap originate from states in the VB and CB edges. The whole band structure evolution is well represented by the evolution of the PP optical spectra upon doping with perchlorate ion (see Figure 7).

V. Summary and Conclusion

The field of conducting polymers has been firmly established. Rapid progress in the past few years has demonstrated that the potential exists for the discovery of new concepts and phenomena as well as the development of new technology.

In this review we have summarized the optical studies of some of the key conducting organic polymers that have become important in recent years. The optical properties of conducting polymers are important to the development of an understanding of the basic electronic structure of the material. The in situ technique described for studying the charge-transfer doping reacions in conducting polymers has made it possible to determine the nature of the charge-storage states as well as to monitor the kinetics of the charge-transfer reaction. Such studies have played an important role in clarifying the chemistry and physics of conducting polymers. In conjugated polymers other than polyacetylene, electrons added or removed from the delocalized π-bonded backbone initially produce polarons (radical ions coupled to a spatially extended distortion of the bond lengths) which subsequently combine to form dianions or dications (spinless bipolarons), respectively. In polyacetylene anions and cations *but not radical anions or radical cations* are produced during charge transfer. The development of an understanding of these novel spinless negative or positive solitons (or charged bond-alternation domain walls) has been a major focus of the theoretical studies of conducting polymers. The study of these bipolarons in polythiophene (or solitons in polyacetylene) has demonstrated that the concepts carry over in detail and that an understanding of the resulting phenomena is possible even for relatively complex systems.

The high-contrast electrochromic phenomenon associated with electrochemical doping and the characteristic changes in absorption spectra shown throughout the review appear to be general features of conducting polymers. The oscillator strength associated with the interband transition prior to doping shifts into the free carrier contribution in the infrared after doping. The effect of such spectral changes depends initially on the magnitude of the energy gap. If E_g is greater than 3 eV, the undoped insulating polymer is transparent (or lightly colored), whereas after doping the conducting polymer is typically highly absorbing in the visible. If, however, E_g is small ($\sim$1–1.5 eV), the undoped polymer will be highly absorbing, whereas after doping the free carrier absorption can be relatively weak in the visible (provided the typical carrier scattering time and mean free path are sufficiently long), rendering the polymers transparent in this visible region of the electromagnetic spectrum.

A principal goal of the field of conducting polymers is to achieve a fundamental understanding of the relationship between chemical structure of the monomer units and electronic properties of the resulting conjugated polymer. With insights described in this review, specific electronic properties should be obtainable by molecular design. Initial success in this direction was the preparation of the 1-eV-gap polymer PITN.

Another result of fundamental importance described in this review was the discovery that polymers that are soluble (and hence processible) in common organic solvents and in water show *the same spectroscopic characteristics in dilute solution* as in the solid state, particularly as a function of doping; i.e., charge storage in the form of dications is *not relegated to a solid state effect* but is an *intrinsic, single-molecule effect.*

The future of the field relies on creative synthesis of new systems and the attainment of completely aligned polymer chains in the solid state. The essential feature required for conducting polymers is conjugated systems with a π-electron band structure. Such polymers can undergo charge-transfer reactions electrochemically or with suitable electron donors or acceptors to provide potential carriers. The mobility of these carriers will be determined by a variety of effects, including chain perfection and crystallinity, obtained by chain alignment.

As powerful and informative as the reviewed in situ spectroscopic technique is, it should never be used without the support from other characterization methods such as elemental analysis (in the case of doping studies), electron spin resonance, NMR, IR, etc. A case in point is the recent report of the preparation of very small band gap semiconducting polymers.[67] A more complete study[68] showed that the true energy gap was in fact relatively large.

Acknowledgments. This research was supported by the Office of Naval Research under contract N00014-83-K-0450.

VI. References

(1) (a) Shirakawa, H.; Louis, E. J.; MacDiarmid, A. G.; Chiang, C. K.; Heeger, A. J. *J. Chem. Soc., Chem. Commun.* **1977**, 578. (b) Chiang, C. K.; Fincher, C. R.; Park, Y. W.; Heeger, A. J.; Shirakawa, H.; Louis, E. J.; Gau, S. C.; MacDiarmid, A. G. *Phys. Rev. Lett.* **1977**, *39*, 1098.
(2) (a) Skotheim, T. J., Ed. *Handbook of Conducting Polymers*; Marcel Dekker: New York, 1986. (b) Etemad, S.; Heeger, A. J.; MacDiarmid, A. G. *Annu. Rev. Phys. Chem.* **1982**, *33*, 443. (c) Bredas, J. L.; Street, G. B. *Acc. Chem. Res.* **1985**, *18*, 309. (d) Green, R. L.; Street, G. B. *Science (Washington, D.C.)* **1984**, *226*, 651.
(3) Ito, T.; Shirakawa, H.; Ikeda, S. *J. Polym. Sci., Polym. Chem. Ed.* **1974**, *12*, 11.
(4) Ito, T.; Shirakawa, H.; Ikeda, S. *J. Polym. Sci.* **1975**, *13*, 1943.

(5) (a) Shirakawa, H.; Ito, T.; Ikeda, S. *Makromol. Chem.* **1978**, *179*, 1565. (b) Naarmann, H. *Synth. Met.* **1987**, *17*, 2233. Naarmann, H.; Theophilou, N. *Synth. Met.* **1987**, *22*, 1. (c) Naarmann, H. 193rd National Meeting of the American Chemical Society, Denver, CO, Apr 5–10, 1987, in Symposium on Conducting Polymers: Their Emergence and Future, sponsored by the Inorganic Division. Basescu, N.; Liu, Z.-X.; Moses, D.; Heeger, A. J.; Naarmann, H.; Theophilou, N. *Nature (London)* **1987**, *327*, 403.
(6) Shirakawa, H.; Ikeda, S. *Synth. Met.* **1979/1980**, *1*, 175.
(7) Karasz, F. E.; Chien, J. C. W.; Galkiewicz, R.; Wnek, G. E.; Heeger, A. J.; MacDiarmid, A. G. *Nature (London)* **1979**, *282*, 286.
(8) Park, Y. W.; Druy, M. A.; Chiang, C. K.; MacDiarmid, A. G.; Heeger, A. J.; Shirakawa, H.; Ikeda, S. *J. Polym. Sci., Polym. Lett. Ed.* **1979**, *17*, 628.
(9) Druy, M. A.; Tsang, C. H.; Brown, N.; Heeger, A. J.; MacDiarmid, A. G. *J. Polym. Sci., Polym. Phys. Ed.* **1980**, *18*, 429.
(10) Ito, T.; Shirakawa, H.; Ikeda, S. *Kobunshi Ronbunshu* **1976**, *33*, 339; *Chem. Abstr.* **1976**, *85*, 78449c.
(11) Akaishi, T.; Miyasaka, K.; Ishikawa, K.; Shirakawa, H.; Ikeda, S. *J. Polym. Sci., Polym. Phys. Ed.* **1980**, *18*, 745.
(12) Fincher, C. R.; Chen, C. E.; Heeger, A. J.; MacDiarmid, A. G.; Hastings, J. B. *Phys. Rev. Lett.* **1982**, *48*, 100.
(13) Peierls, R. E. *Quantum Theory of Solids*; Oxford University Press: London, 1955; p 108.
(14) Devreese, J. T.; Evrard, R. P.; Van Doren, V. E., Eds. *Highly Conducting One-Dimensional Solids*; Plenum: New York, 1978 (contains several reviews on this topic).
(15) (a) Su, W. P.; Schrieffer, J. R.; Heeger, A. J. *Phys. Rev. Lett* **1979**, *42*, 1698. (b) Su, W. P.; Schrieffer, J. R.; Heeger, A. J. *Phys. Rev. B* **1981**, *22*, 2099.
(16) Rice, M. J. *Phys. Lett. A* **1979**, *71*, 152.
(17) Takayama, H.; Lin-Liu, Y. R.; Maki, K. *Phys. Rev. B* **1980**, *21*, 2388.
(18) (a) Brazovskii, S. *JETP Lett.* **1979**, *28*, 656. (b) Brazovskii, S. *JETP* **1980**, *78*, 677.
(19) (a) Heeger, A. J.; MacDiarmid, A. G. Proceedings of the International Conference on Low Dimensional Synthetic Metals, Helsingor, Denmark, *Chem. Scr.* **1981**, *17*, 115. Proceedings of the International Conference on Low Dimensional Conductors, Boulder, CO, *Mol. Cryst. Liq. Cryst.* **1981**, *77*, 1. (b) Alcacer, L., Ed. *Phys. Chem. Low Dimens. Solids* **1980**, *393*, 353.
(20) Etemad, S.; Heeger, A. J.; Lauchlan, L.; Chung, T.-C.; MacDiarmid, A. G. Proceedings of the International Conference on Low Dimensional Conductors, Boulder, CO, *Mol. Cryst. Liq. Cryst.* **1981**, *77*, 43.
(21) Dall'Olio, A.; Dascola, Y.; Varacco, V.; Bocchi, C. R. *C. R. Seances Acad. Sci., Ser. C* **1968**, *267*, 433.
(22) Kanazawa, K. K.; Diaz, A. F.; Geiss, R. H.; Gill, W. D.; Kwak, J. F.; Logan, J. A.; Rabolt, J. F.; Street, G. B. *J. Chem. Soc., Chem. Commun.* **1979**, 854.
(23) Bryce, M. R.; Chissel, A.; Kathirgamanathanan, P.; Parker, D.; Smith, N. R. M. *J. Chem. Soc., Chem. Commun.* **1987**, 466.
(24) Feldblum, A.; Kaufman, J. H.; Etemad, S.; Heeger, A. J.; Chung, T.-C.; MacDiarmid, A. G. *Phys. Rev. B* **1982**, *26*, 815.
(25) Chung, T.-C.; Kaufman, J. H.; Heeger, A. J.; Wudl, F. *Phys. Rev. B* **1984**, *30*, 702.
(26) Roth, S.; Ehringer, K.; Menke, K.; Peo, M.; Schweizer, R. J. *J. Phys. (Paris), Suppl.* **1983**, *C3*, 69.
(27) (a) Nigrey, P. J.; MacDiarmid, A. G.; Heeger, A. J. *J. Chem. Soc., Chem. Commun.* **1979**, 594. (b) Nigrey, P. J.; McInnes, D.; Nairns, D. P.; MacDiarmid, A. G.; Heeger, A. J. *J. Electrochem. Soc.* **1981**, *128*, 1651. (c) Nigrey, P. J.; MacDiarmid, A. G.; Heeger, A. J. Proceedings of the International Conference on Low Dimensional Conductors, Boulder, CO, *Mol. Cryst. Liq. Cryst.* **1982**, *83*, 1341.
(28) McInnes, D.; Druy, M. R.; Nigrey, P. J.; Nairns, D. P.; MacDiarmid, A. G.; Heeger, A. J. *J. Chem. Soc., Chem. Commun.* **1981**, 317.
(29) Feldblum, A.; Kaufman, J. H.; Etemad, S.; Heeger, A. J.; Chung, T.-C.; MacDiarmid, A. G. *Phys. Rev. B* **1982**, *26*, 815.
(30) (a) Kaufman, J. H.; Kaufer, J. W.; Heeger, A. J.; Kaner, R.; MacDiarmid, A. G. *Phys. Rev. B* **1982**, *26*, 4. (b) Kaufman, J. H.; Chung, T.-C.; Heeger, A. J. *Solid State Commun.* **1983**, *47*, 585. (c) Kaufman, J. H.; Chung, T. C.; Heeger, A. J. *J. Electrochem. Soc.* **1984**, *131*, 2092.
(31) Fincher, C. R.; Ozaki, M.; Heeger, A. J.; MacDiarmid, A. G. *Phys. Rev. B* **1979**, *19*, 4140.
(32) Etemad, S.; Pron, A.; Heeger, A. J.; MacDiarmid, A. G.; Mele, E. J.; Rice, M. J. *Phys. Rev. B* **1981**, *23*, 5137.
(33) Blanchet, G. B.; Fincher, C. R.; Chung, T.-C.; Heeger, A. J. *Phys. Rev. Lett.* **1983**, *50*, 1938.
(34) Blanchet, G. B.; Fincher, C. R.; Heeger, A. J. *Phys. Rev. Lett.* **1983**, *51*, 2132.
(35) Vardeny, Z.; Orenstein, J.; Baker, G. L. *Phys. Rev. Lett.* **1983**, *50*, 2032.
(36) Flood, J. D.; Heeger, A. J. *Phys. Rev. B* **1983**, *28*, 2356.
(37) Suzuki, N.; Ozaki, M.; Etemad, S.; Heeger, A. J.; MacDiarmid, A. G. *Phys. Rev. Lett.* **1980**, *45*, 1209; erratum, *Phys. Rev. Lett.* **1980**, *45*, 1483.
(38) Gardini, G. P. *Adv. Heterocycl. Chem.* **1973**, *15*, 67.
(39) Street, G. B.; Clarke, T. C.; Krounbi, M.; Kanazawa, K.; Lee, V.; Pfluger, P.; Scott, J. C.; Weiser, G. *Mol. Cryst. Liq. Cryst.* **1982**, *83*, 253.
(40) Jones, R. A.; Bean, G. P. *Chemistry of Pyrroles*; Academic Press: New York, 1977; p 460.
(41) Yakushi, K.; Lauchlan, L. J.; Clarke, T. C.; Street, G. B. *J. Chem. Phys.* **1983**, *79*, 4774.
(42) Kaufman, J. H.; Colaneri, N.; Scott, J. C.; Street, G. B. *Phys. Rev. Lett.* **1984**, *53*, 1005.
(43) Brêdas, J. L.; Chance, R. R.; Silbey, R. *Mol. Cryst. Liq. Cryst.* **1981**, *77*, 319; *Phys. Rev. B: Condens. Matter* **1982**, *26*, 5843.
(44) Bredas, J. L.; Scott, J. C.; Yakushi, K.; Street, G. B. *Phys. Rev. B: Condens. Matter* **1984**, *30*, 1023.
(45) (a) Gazard, M.; Dubois, J. C.; Champagne, M.; Garnier, F.; Tourillor, G. *J. Phys. (Paris), Colloq.* **1983**, *C3*, 537. (b) Garnier, F.; Tourillon, G.; Gazard, M.; Dubois, J. C. *J. Electroanal. Chem.* **1983**, *148*, 299. (c) Druy, M. A.; Seymour, R. J. *J. Phys. (Paris), Colloq.* **1983**, *C3*, 595.
(46) Kaneto, K.; Kohno, Y.; Yoshino, K. *Mol. Cryst.* liq. *Cryst.* **1985**, *118*, 217.
(47) (a) Wudl, F.; Kobayashi, M.; Heeger, A. J. *J. Org. Chem.* **1984**, *49*, 3382. (b) Kobayashi, M.; Colaneri, N.; Boysel, M.; Wudl, F.; Heeger, A. J. *J. Chem. Phys.* **1985**, *82*, 5717. (c) Colaneri, N.; Kobayashi, M.; Heeger, A. J.; Wudl, F. *Synth. Met.* **1986**, *14*, 45. (d) Bredas, J. L.; Heeger, A. J.; Wudl, F. *J. Chem. Phys.* **1986**, *85*, 4673. (e) Yashima, H.; Kobayashi, M.; Lee, K. B.; Chung, D.; Heeger, A. J.; Wudl, F. *J. Electrochem. Soc., Electrochem. Sci. Tecnol.* **1987**, 46.
(48) Feldblum, A.; Kaufman, J.; Etemad, S.; Heeger, A. J.; MacDiarmid, A. G. *Phys. Rev. B* **1982**, *26*, 815.
(49) (a) Moses, D.; Denenstein, A.; Pron, A.; Heeger, A. J.; MacDiarmid, A. G. *Solid State Commun.* **1980**, *36*, 219. (b) Park, Y. W.; Heeger, A. J.; Druy, M. A.; MacDiarmid, A. G. *J. Chem. Phys.* **1980**, *73*, 946. (c) Ikenaka, S.; Kaufer, J.; Woerner, T.; Pron, A.; Druy, M.; Sivak, A.; Heeger, A. J.; MacDiarmid, A. G. *Phys. Rev. Lett.* **1980**, *45*, 1123.
(50) (a) Frommer, J. E. *Acc. Chem. Res.* **1986**, *19*, 2. (b) Frommer, J. E.; Elsenbaumer, R. L.; Chance, R. R. *Org. Coat. Appl. Polym. Sci. Proc.* **1983**, *48*, 552. (c) Frommer, J. E.; Elsenbaumer, R. L.; Chance, R. R. *Polymers in Electronics*; Davidson, T., Ed.; American Chemical Society: Washington, DC, 1984; ACS Symp. Ser. No. 242, p 447.
(51) Jenekhe, S. A.; Wellinghoff, S. T.; Reed, J. F. *Mol. Cryst. Liq. Cryst.* **1984**, *105*, 175.
(52) Sato, M.; Tanaka, S.; Kaeriyama, K. *J. Chem. Soc., Chem. Commun.* **1986**, 873.
(53) (a) Jen, K. Y.; Oboodi, R.; Elsenbaumer, R. L. *Polym. Mater. Sci. Eng.* **1985**, *53*, 79. (b) Jen, K. Y.; Miller, G. G.; Elsenbaumer, R. L. *J. Chem. Soc., Chem. Commun.* **1986**, 1346. (c) Elsenbaumer, R. L.; Jen, K. Y.; Oboodi, R. *Synth. Met.* **1986**, *15*, 169.
(54) (a) Hotta, S.; Rughooputh, S. D. D. V.; Heeger, A. J.; Wudl, F. *Macromolecules* **1987**, *20*, 212. (b) Nowak, M.; Rughooputh, S. D. D. V.; Hotta, S.; Heeger, A. J. *Macromolecules* **1987**, *20*, 965. (c) Rughooputh, S. D. D. V.; hotta, S.; Heeger, A. J.; Wudl, F. *J. Polym. Sci., Polym. Phys. Ed.* **1987**, *25*, 1071.
(55) Patil, A. O.; Ikenoue, Y.; Basescu, N.; Colaneri, N.; Chen, J.; Wudl, F.; Heeger, A. J. *Synth. Met.* **1987**, *20*, 151.
(56) Patil, A. O.; Ikenoue, Y.; Wudl, F.; Heeger, A. J. *J. Am. Chem. Soc.* **1987**, *109*, 1858.
(57) (a) Heeger, A. J. *Comments Solid State Phys.* **1981**, *10*, 53. (b) Su, W. P.; Schrieffer, J. R. *Proc. Natl. Acad. Sci. U.S.A.* **1980**, *77*, 5626. (c) Su, Z.; Yu, L. *Phys. Rev. B* **1983**, *27*, 5199. (d) Brazovskii, S. A.; Kirova, N. *JETP Lett.* **1981**, *33*, 4.
(58) (a) Weinberger, B. R.; Ehrenfreund, R.; Heeger, A. J.; MacDiarmid, A. G. *J. Chem. Phys.* **1980**, *72*, 4749. (b) Nechtschein, M.; Devreaux, F.; Green, R. L.; Clark, T. C.; Street, G. B. *Phys. Rev. Lett.* **1980**, *44*, 356.
(59) Schaffer, H. E.; Heeger, A. J. *Solid State Commun.* **1986**, *59*, 415.
(60) Melê, E. J. *Solid State Commun.* **1982**, 44, 827; *Synth. Met.* **1984**, *9*, 207.
(61) Fesser, K.; Bishop, A. R.; Champbell, D. K. *Phys. Rev. B* **1983**, *27*, 4804.
(62) Moses, D.; Feldblum, A.; Denenstein, A.; Ehrenfreund, E.; Chung, T.-C.; Heeger, A. J.; MacDiarmid, A. G. *Phys. Rev. B* **1982**, *26*, 3361.
(63) Moraes, F.; Davidov, D.; Kobayashi, M.; Chung, T.-C.; Chen, J.; Heeger, A. J.; Wudl, F. *Synth. Met.* **1985**, *10*, 169.
(64) Chung, T.-C.; Feldblum, A.; Heeger, A. J.; MacDiarmid, A. G. *J. Chem. Phys.* **1981**, *47*, 5504.
(65) Chung, T.-C.; Moraes, F.; Flood, J. D.; Heeger, A. J. *Phys. Rev. B* **1983**, *29*, 2341.
(66) Kaneto, K.; Kohno, Y.; Yoshino, K.; Inuishi, Y. *J. Chem. Soc., Chem. Commun.* **1983**, 382.
(67) Jenekhe, S. A. *Nature (London)* **1986**, *322*, 345. Jenekhe, S. A. *Macromolecules* **1986**, *19*, 2663. Jenekhe, S. A. *Polym. Prepr.* **1986**, *17*, 74.
(68) Patil, A. O.; Wudl, F. *Macromolecules*, in press. Patil, A. O.; Wudl, F. *Polym. Prepr.* **1987**, *28*, 341.